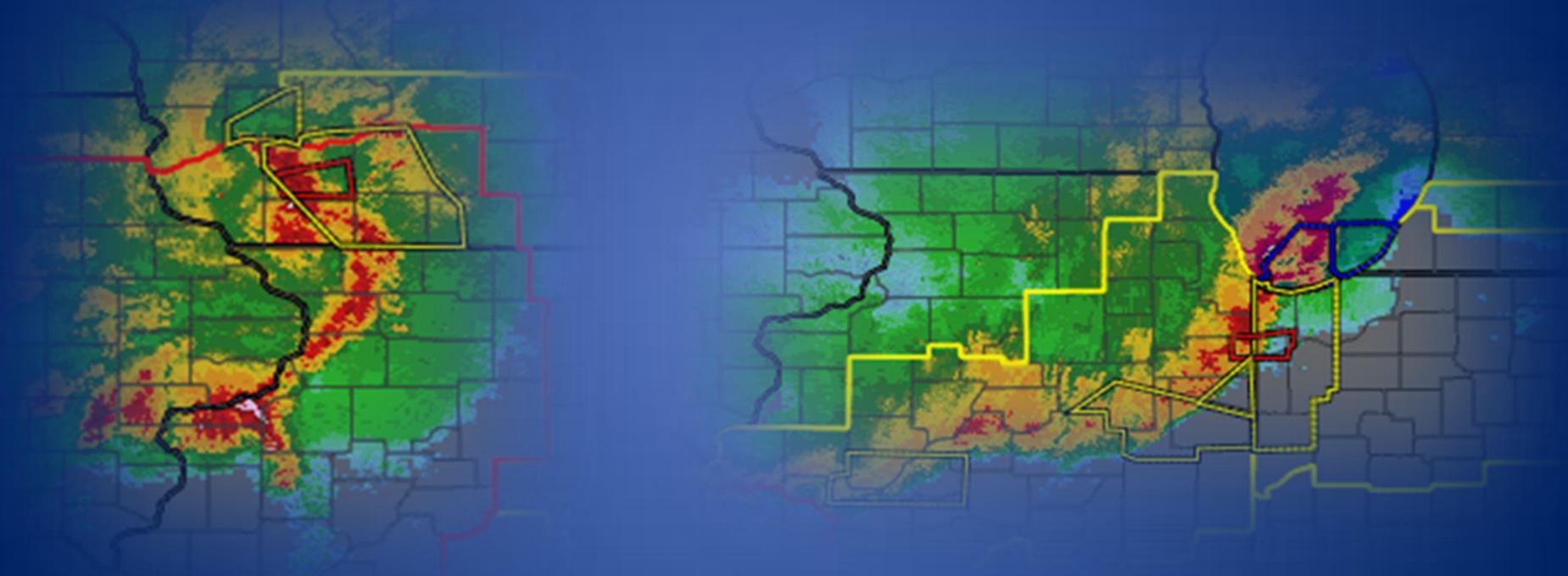


Evolution of the 30 June 2014 Double Derecho Event in Northern Illinois & Northwest Indiana



Eric Lenning, Matthew Friedlein, & Richard Castro
NOAA/National Weather Service – Chicago, IL

Anthony Lyza & Kevin Knupp
Atmospheric Sciences Department, University of Alabama in Huntsville

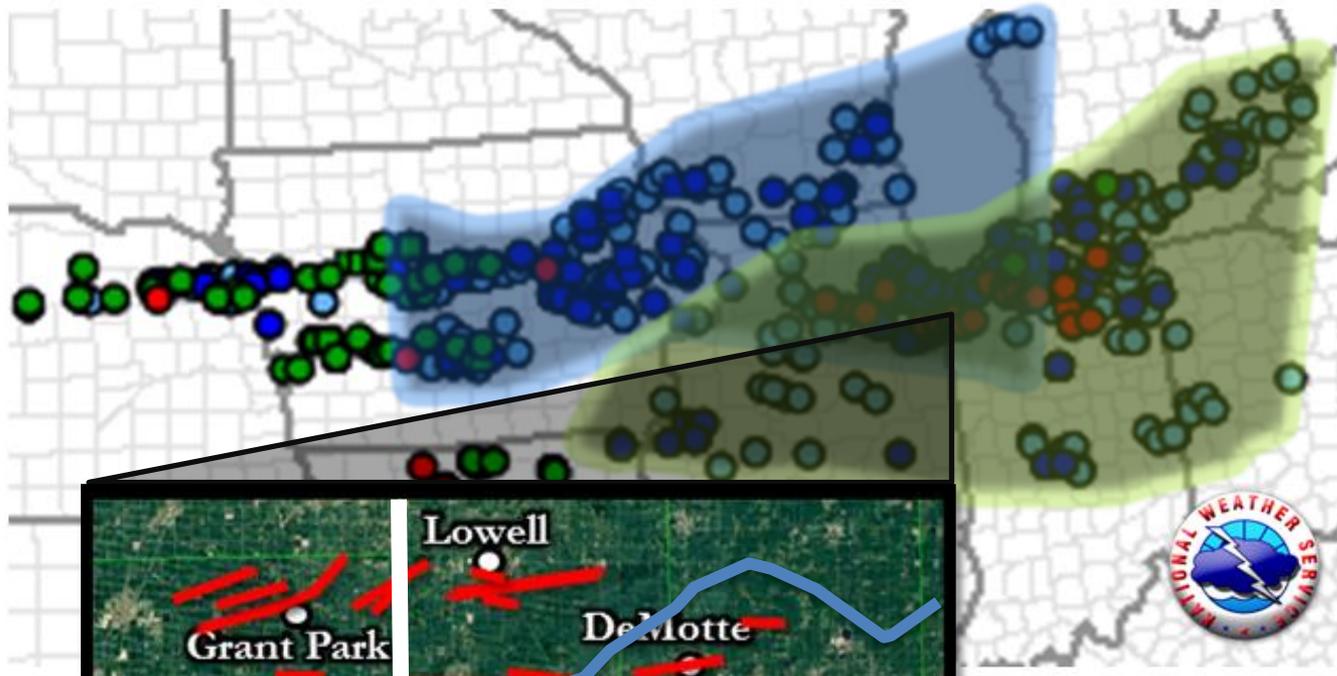
23rd Great Lakes Operational Meteorology Workshop: August 24-27, 2015

Outline & Takeaways

- *Quick* event summary
- *Brief* synoptic and mesoscale evolution
- **Why was second derecho more intense, and a prolific QLCS tornado producer?**
 - What from the first MCS actually helped?
 - Storm scale factors

Severe Storm Reports on June 30th

- Tornado
- Hail
- Wind Gust
- Wind Damage



First Derecho

Time: 1:45 pm – 7:30 pm CDT

Wind: 112

Tornadoes: 2

Hail: 28

Second Derecho

Time: 8 pm – 2 am CDT

Wind: 119

Tornadoes: 29

Hail: 3

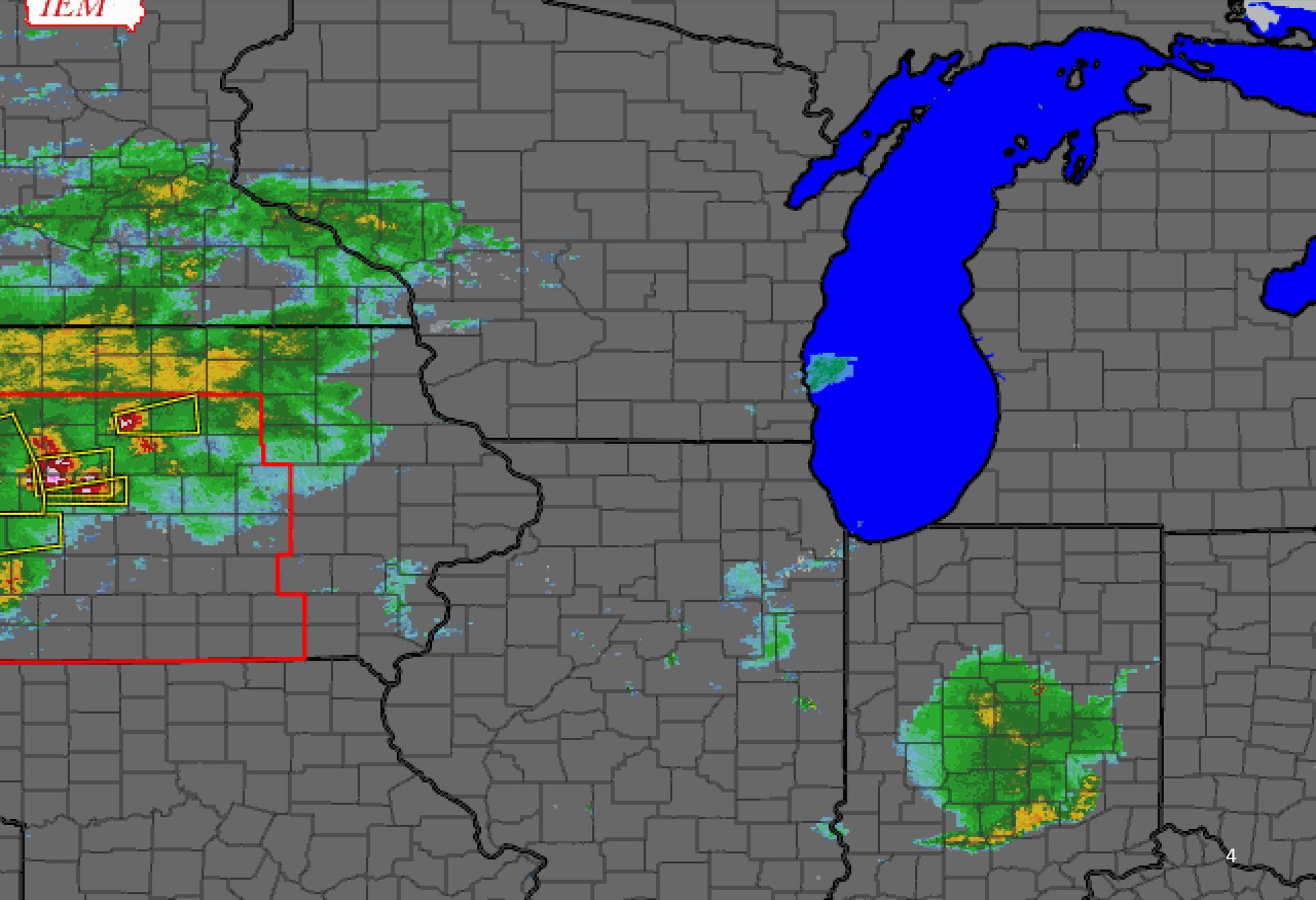
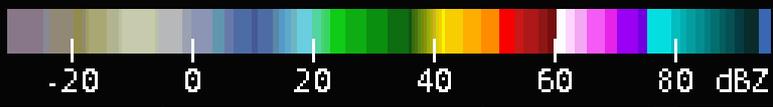
Timeline across Chicago CWA

21-02 UTC and 02-04 UTC



NEXRAD Base Reflectivity

30 June 2014 12:00 PM CDT







© Windy Acres Photography



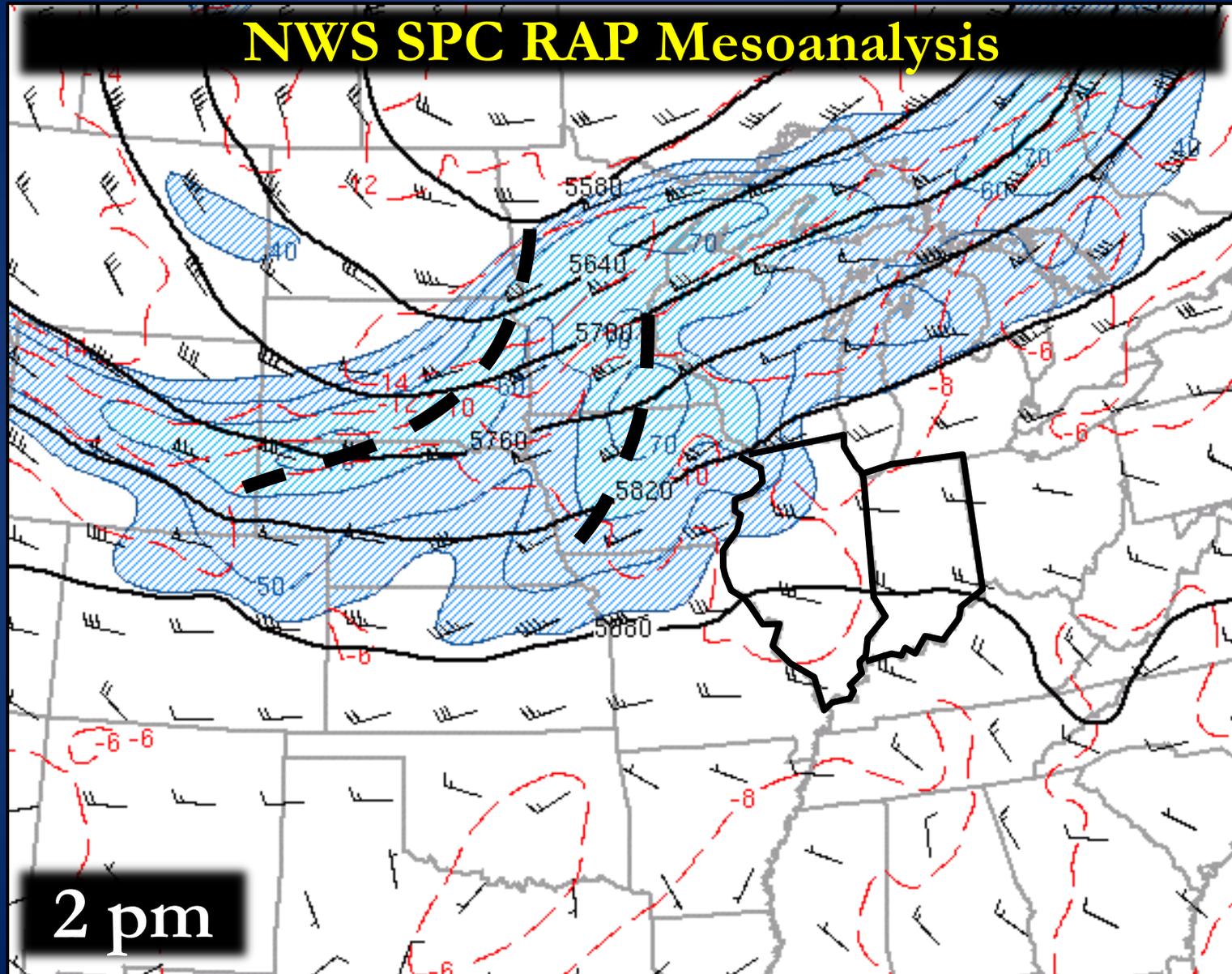
Courtesy of ABC7 Chicago



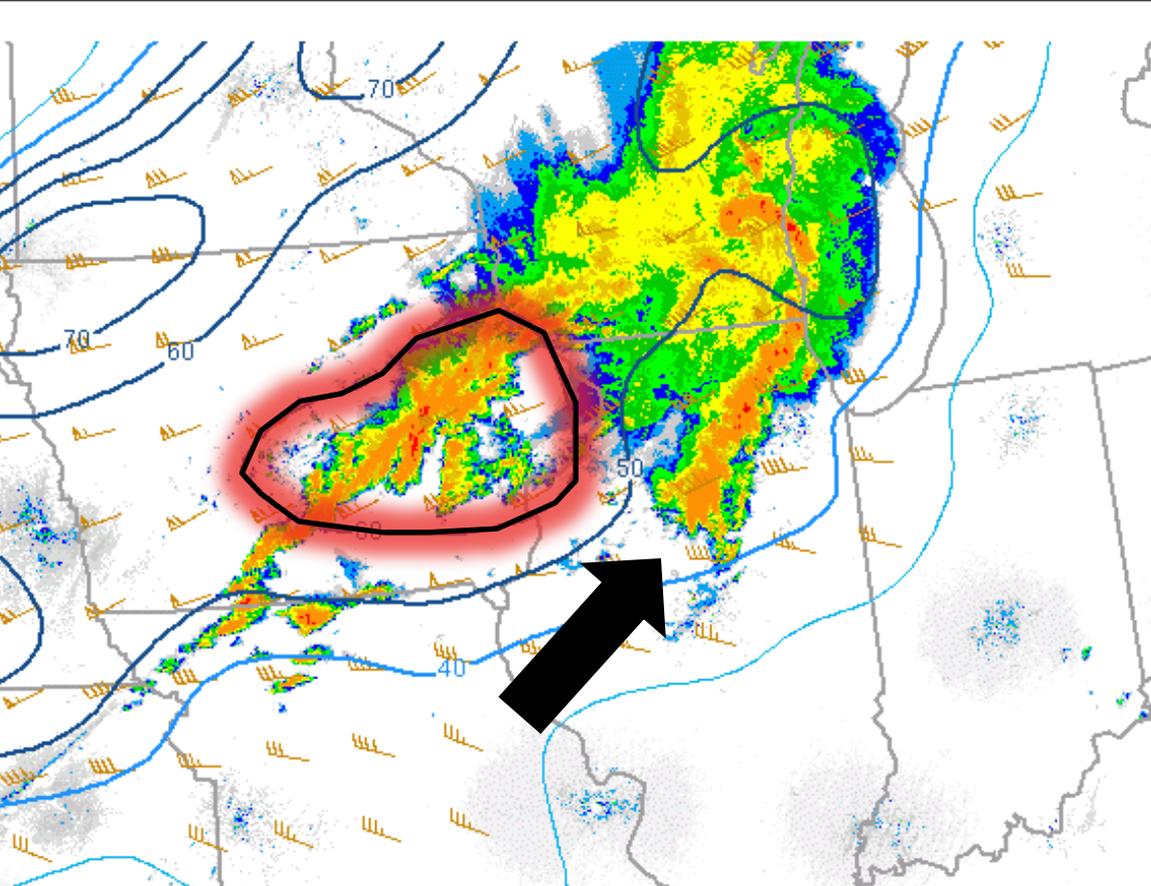
Earlville, IL

First Tornado of Second Derecho

The Synoptic Environment of 30 June 2014: 500 mb



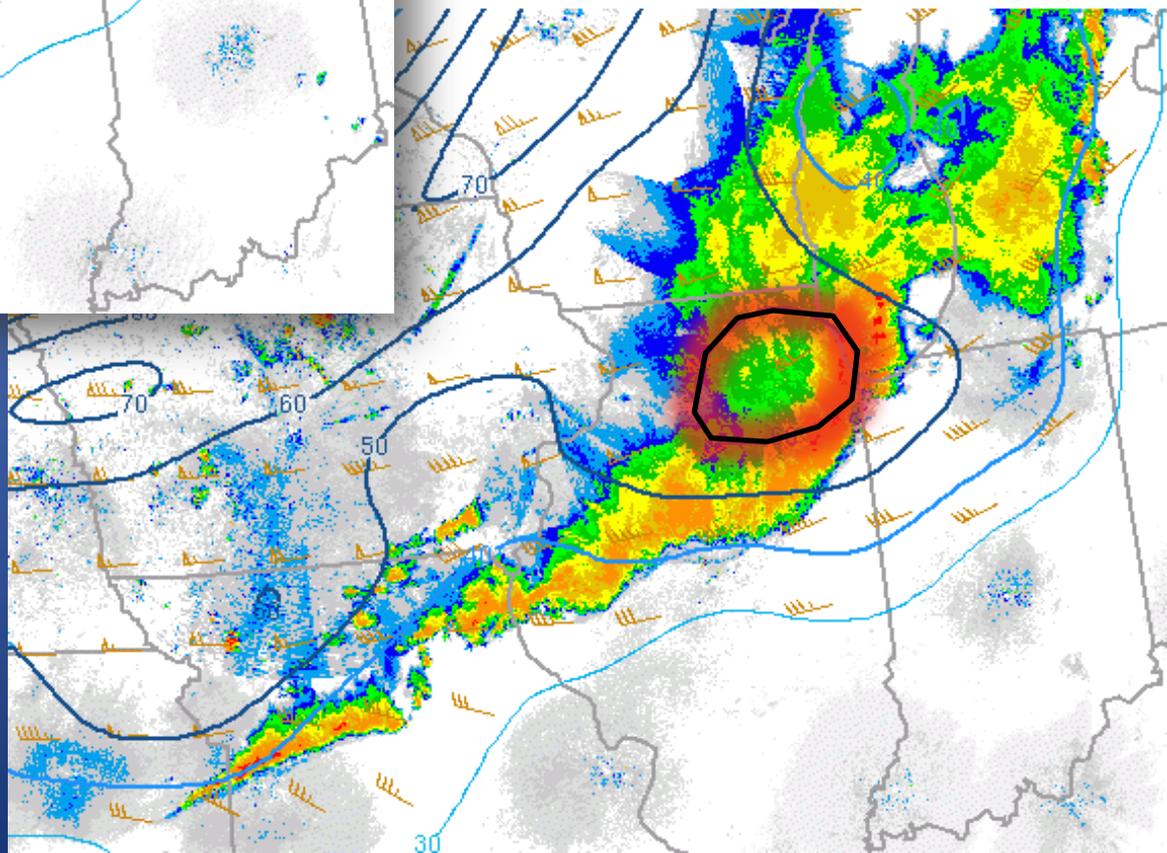
<http://www.spc.noaa.gov/exper/mesoanalysis/>



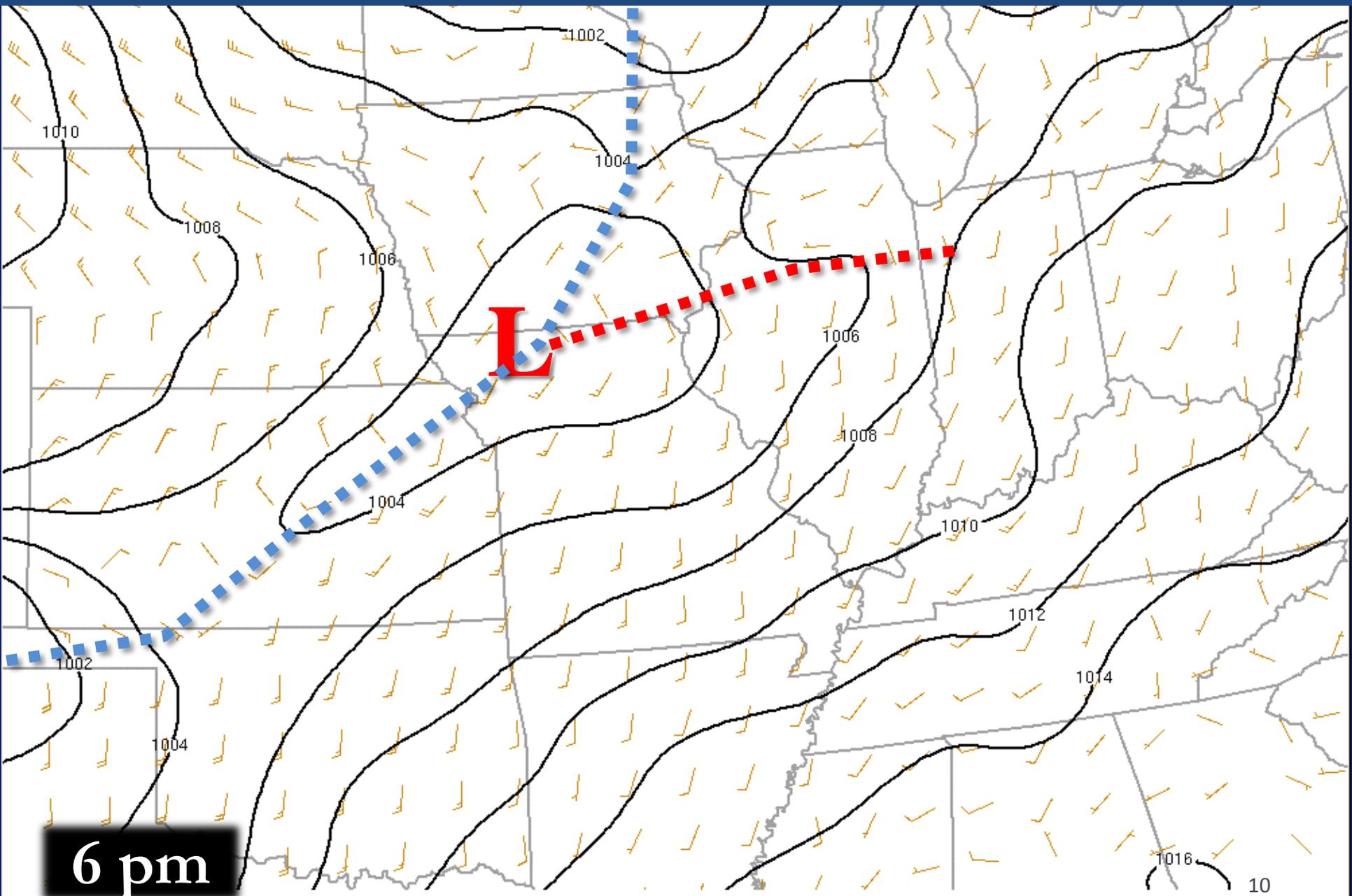
SECOND LINE
03Z 0-6km SHEAR:
25-30 m/s



FIRST LINE
23Z 0-6km SHEAR:
20-25 m/s

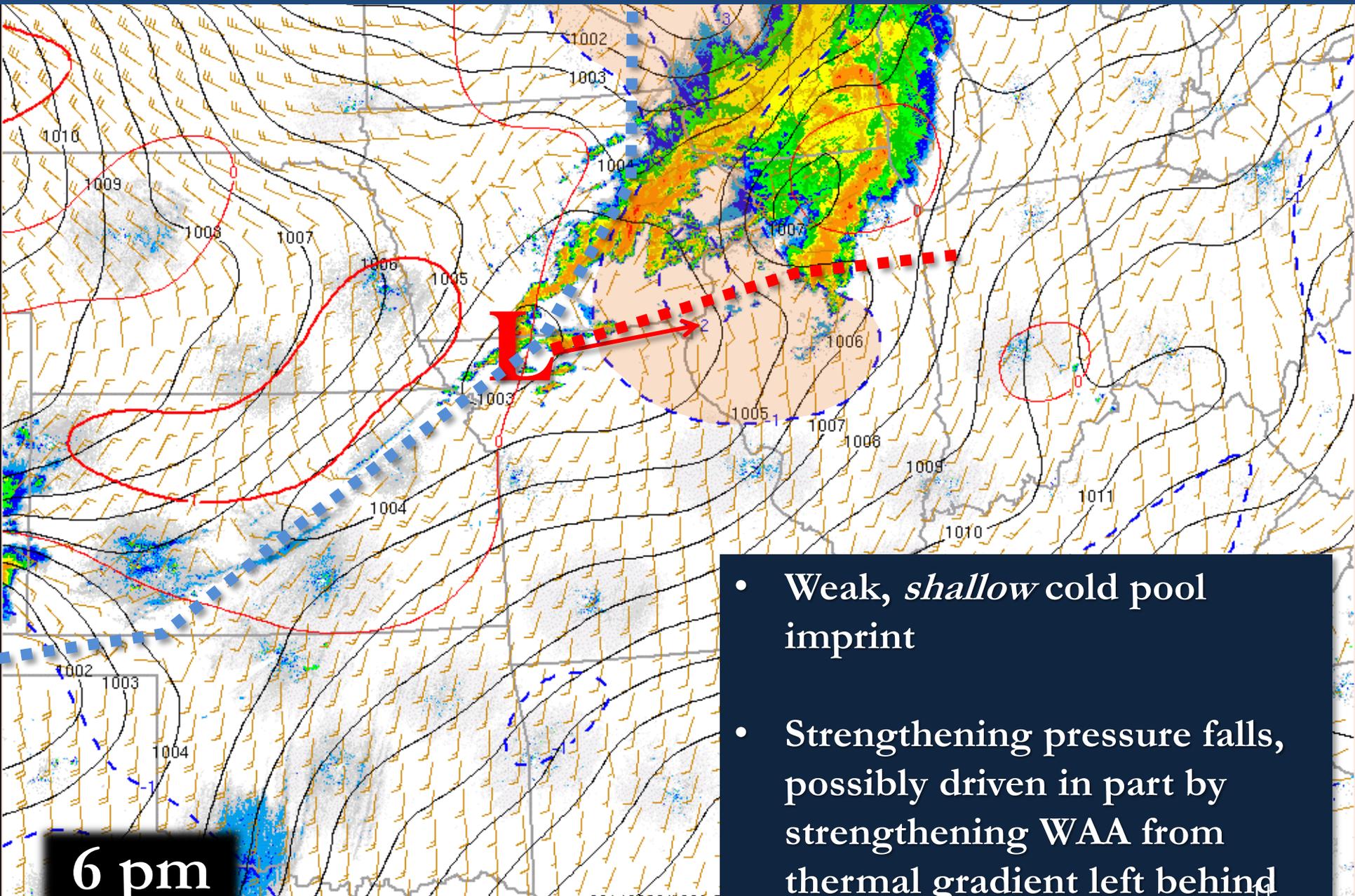


The Synoptic Environment of 30 June 2014: MSLP



140630/2300 MSL Pressure and surface wind

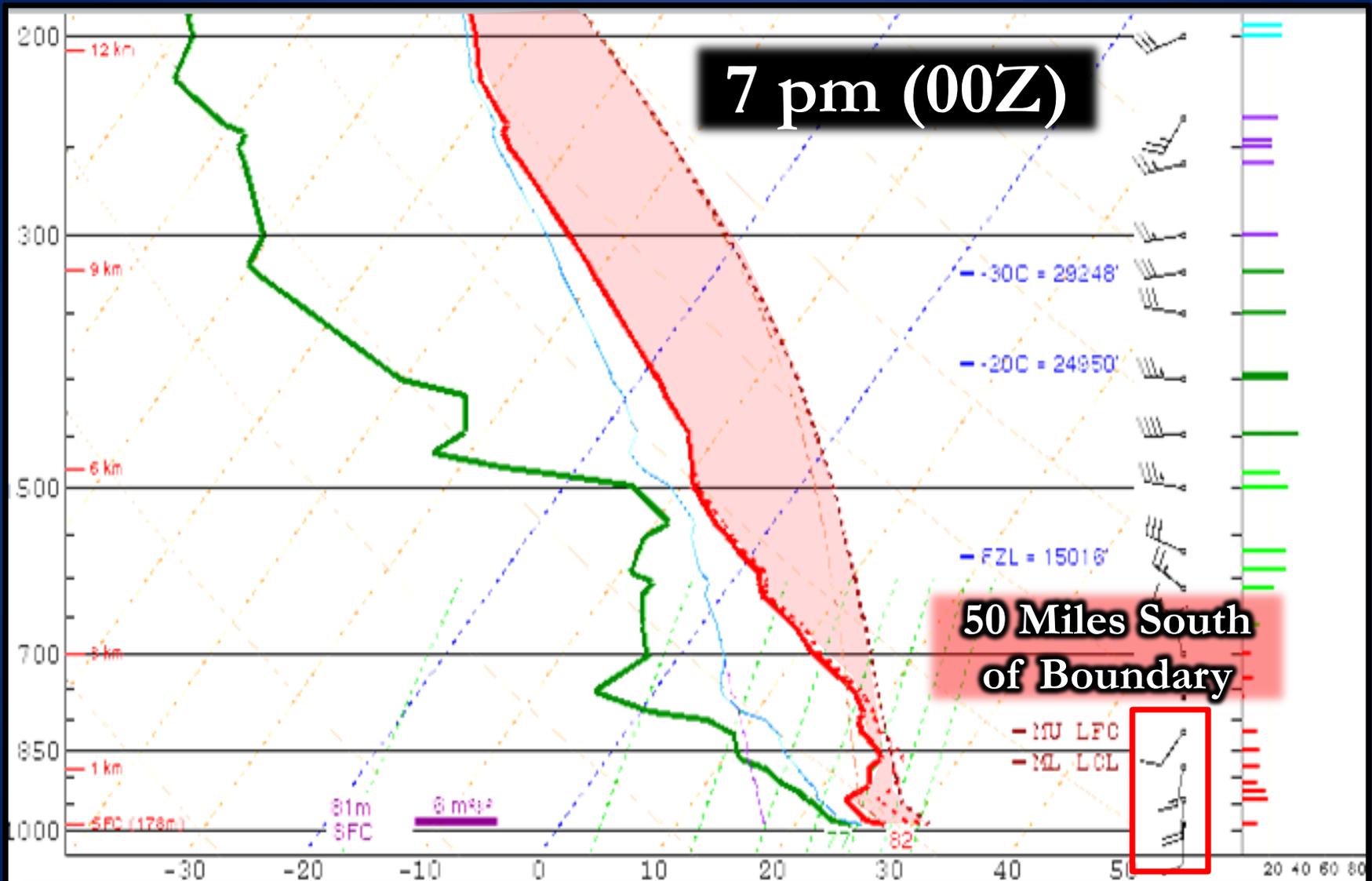
The Synoptic Environment of 30 June 2014: MSLP & 2h Change



- Weak, *shallow* cold pool imprint
- Strengthening pressure falls, possibly driven in part by strengthening WAA from thermal gradient left behind

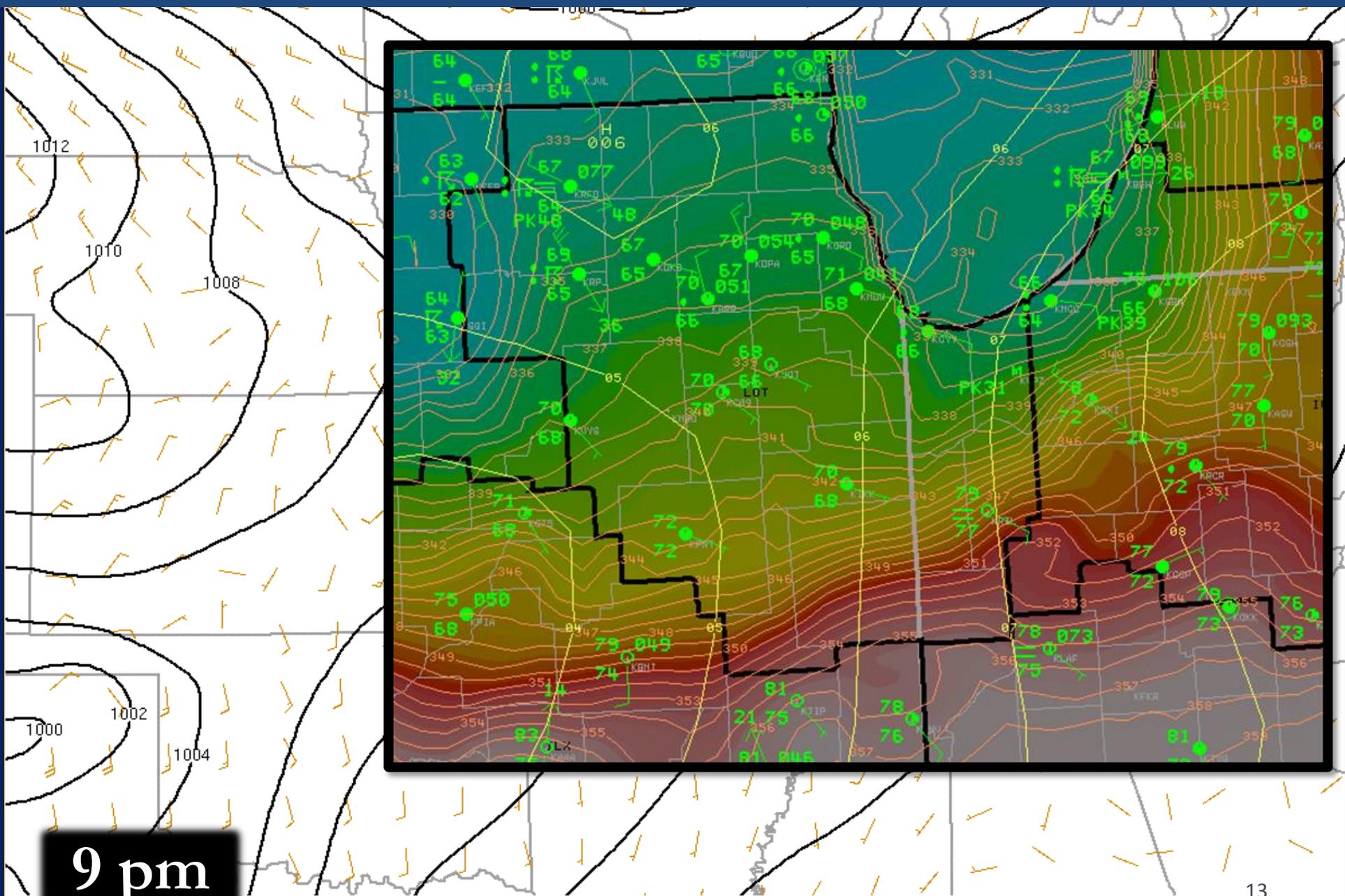
6 pm

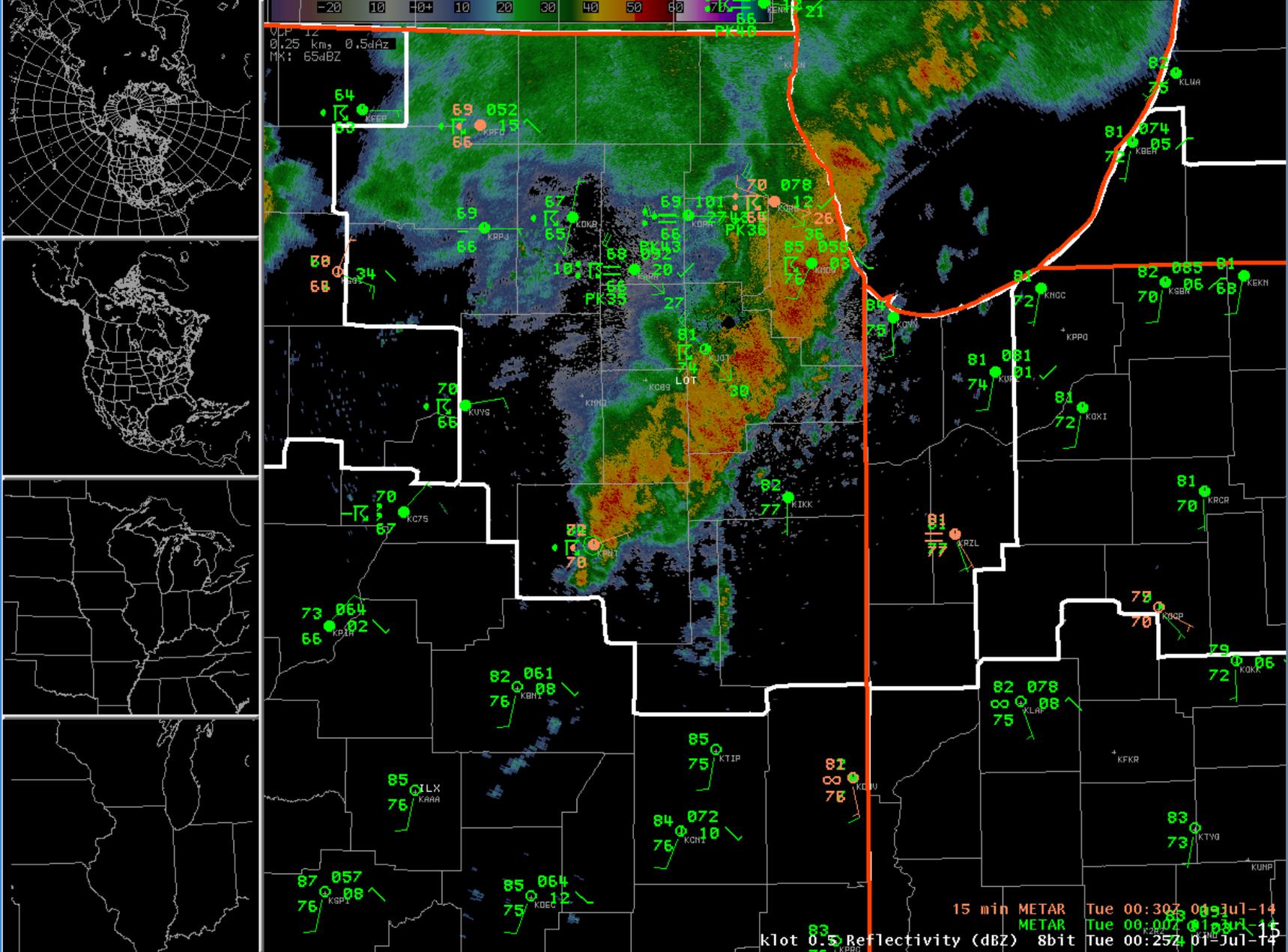
The Synoptic Environment of 30 June 2014: ILX Sounding



PARCEL	CAPE	CINH	LCL	LI	LFC	EL	SRH(m2/s2)	Shear(kt)	MnWind	SRW	
SURFACE	4880	-8	358m	-11	1627m	48080'					
MIXED LAYER	1837	-215	1112m	-8	2997m	41913'					
POST SURFACE	3163	-33	1792m	-9	2565m	46500'					
MU (989 mb)	4880	-8	358m	-11	1627m	48080'					
							SFC - 1 km	27	3	186/16	166/29
							SFC - 3 km	-16	-22	195/8	162/22
							Eff Inflow Layer	6	2	181/14	162/27
							SFC - 6 km		34	258/9	178/14

The Synoptic Environment of 30 June 2014: MSLP & Theta-E





15 min METAR Tue 00:30Z 01 Jul-14
METAR Tue 00:07Z 01 Jul-14
klot 0.5 Reflectivity (dBZ) 8bit Tue 00:25Z 01 Jul-14

Valid time seq

WFO

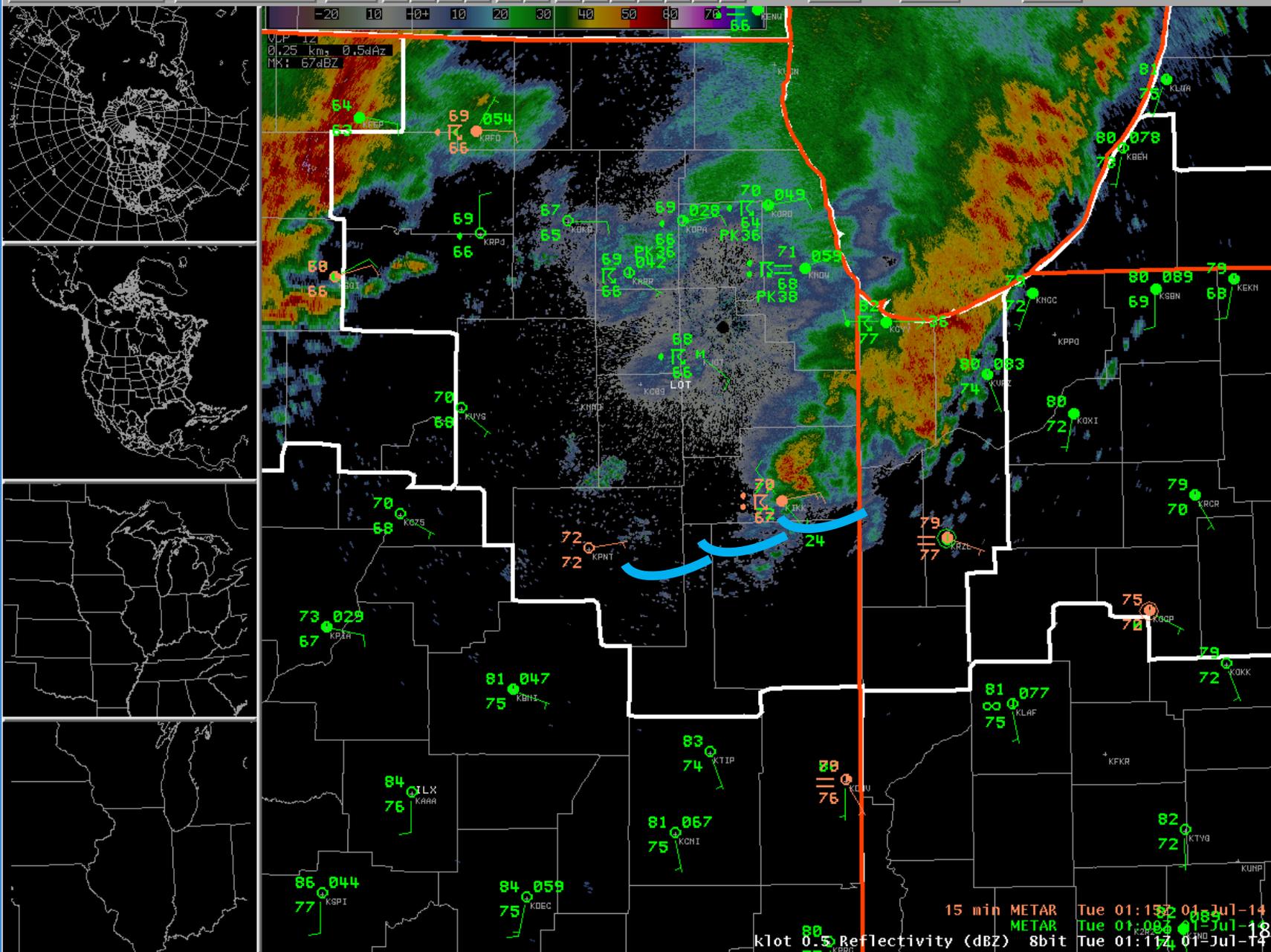
Clear

Navigation icons

Frames: 64

Mag: 1

Density: 1



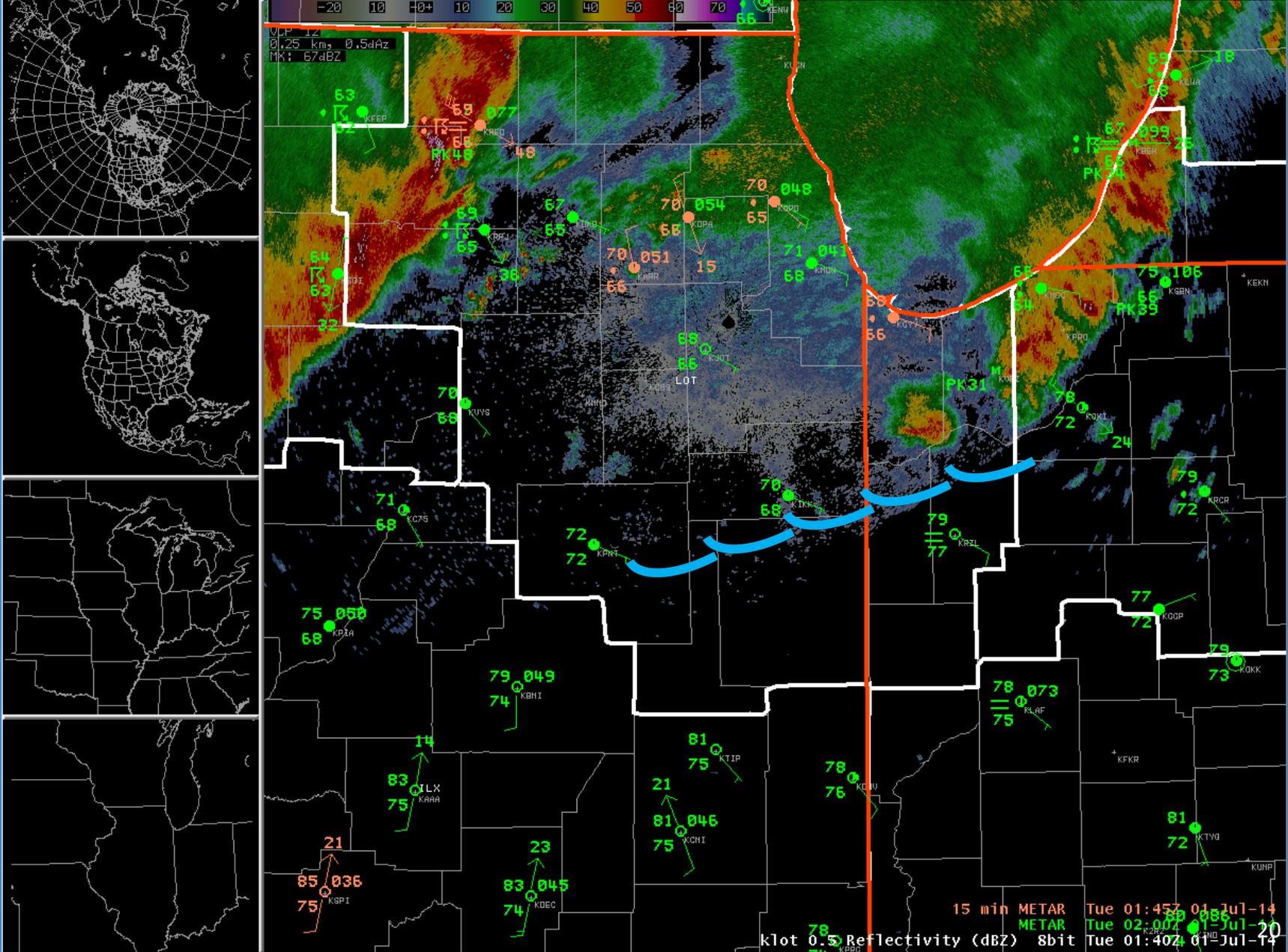
VPP 12
0.25 km 0.5dBz
MK: 67dBZ

15 min METAR Tue 01:15Z 01-Jul-14
METAR Tue 01:09Z 01-Jul-14
klot 0.5 Reflectivity (dBZ) 8bit Tue 01:17Z 01-Jul-14

Status: [dropdown]

Radar: [dropdown]

Frames: 9 Time: 02:10 Z 01-Jul-14



Valid time seq

WFO

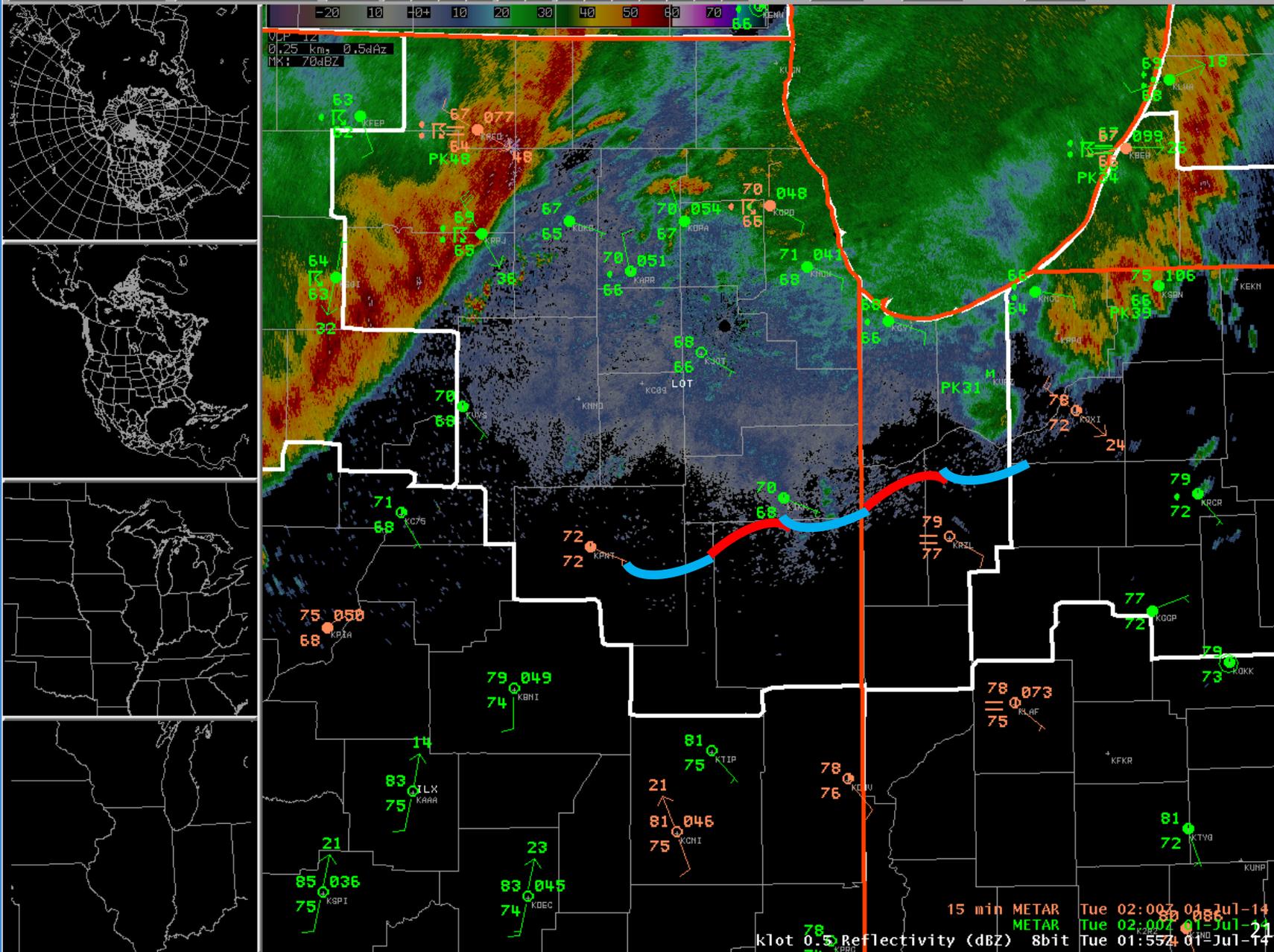
Clear

Navigation icons: back, forward, refresh, zoom in, zoom out, pan, etc.

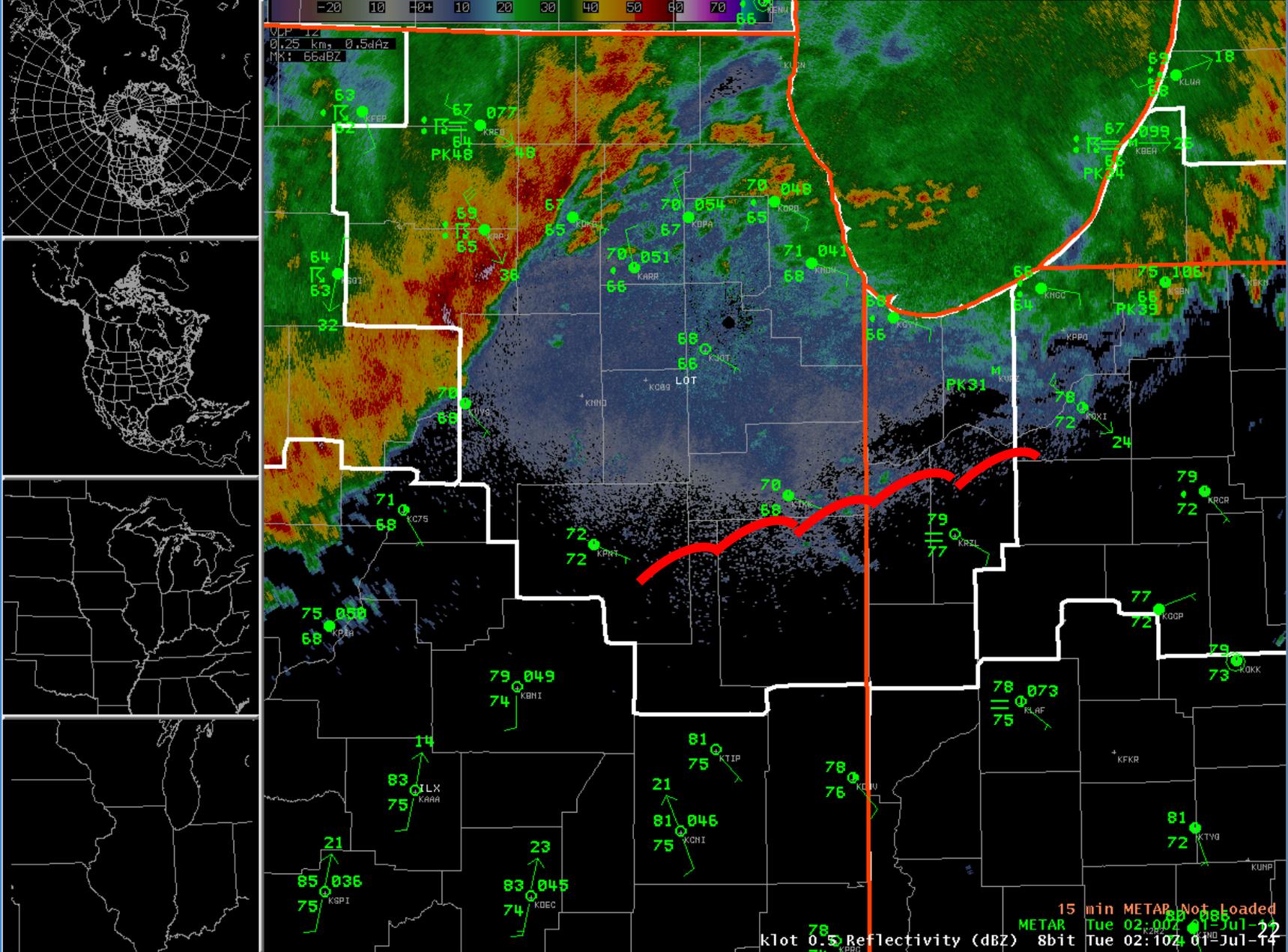
Frames: 64

Mag: 1

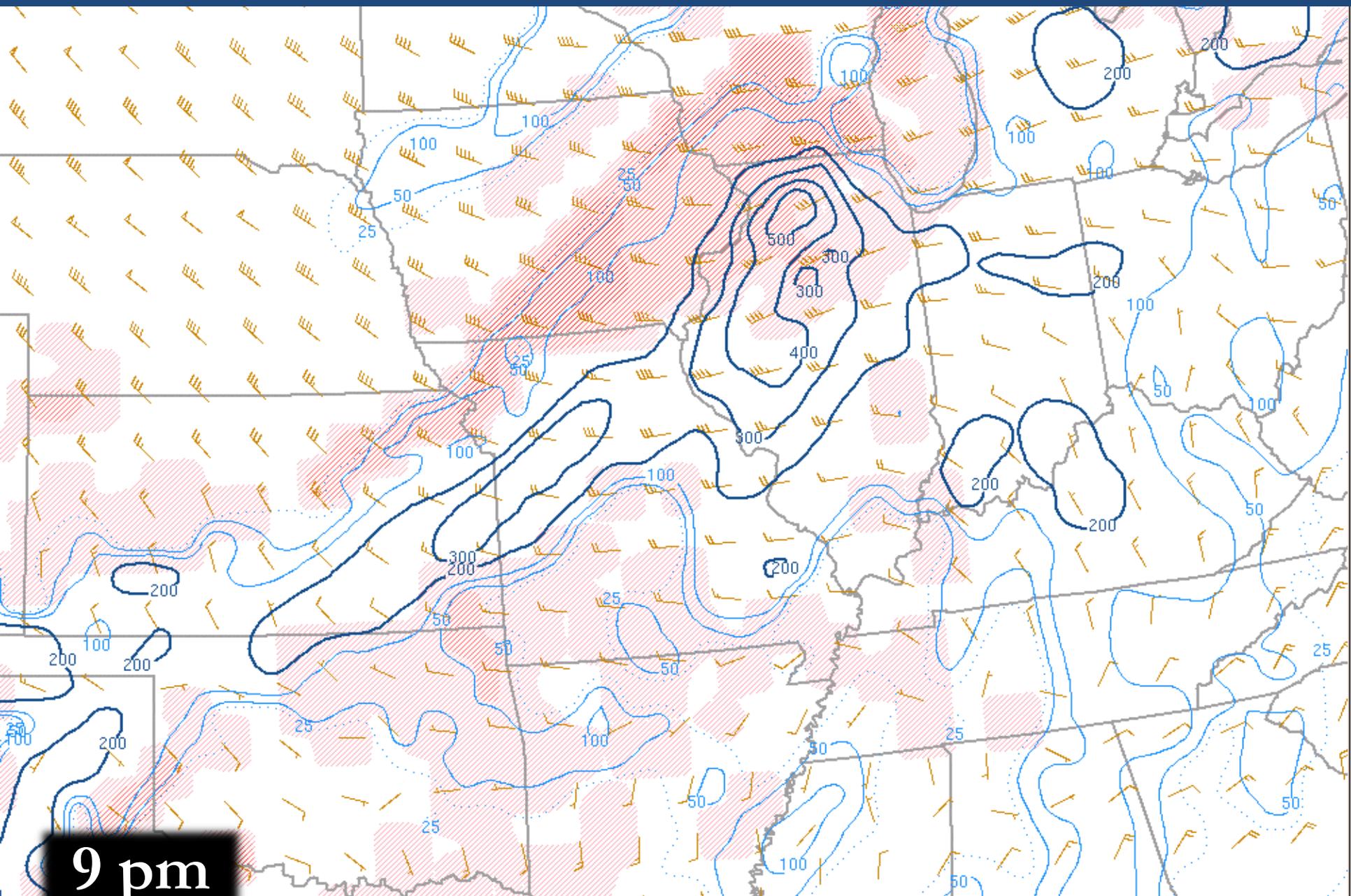
Density: 1



15 min METAR Tue 02:00Z 01-Jul-14
 METAR Tue 02:00Z 01-Jul-14
 Tue 01:55Z 01-Jul-14
 klot 0.5 Reflectivity (dBZ) 8bit



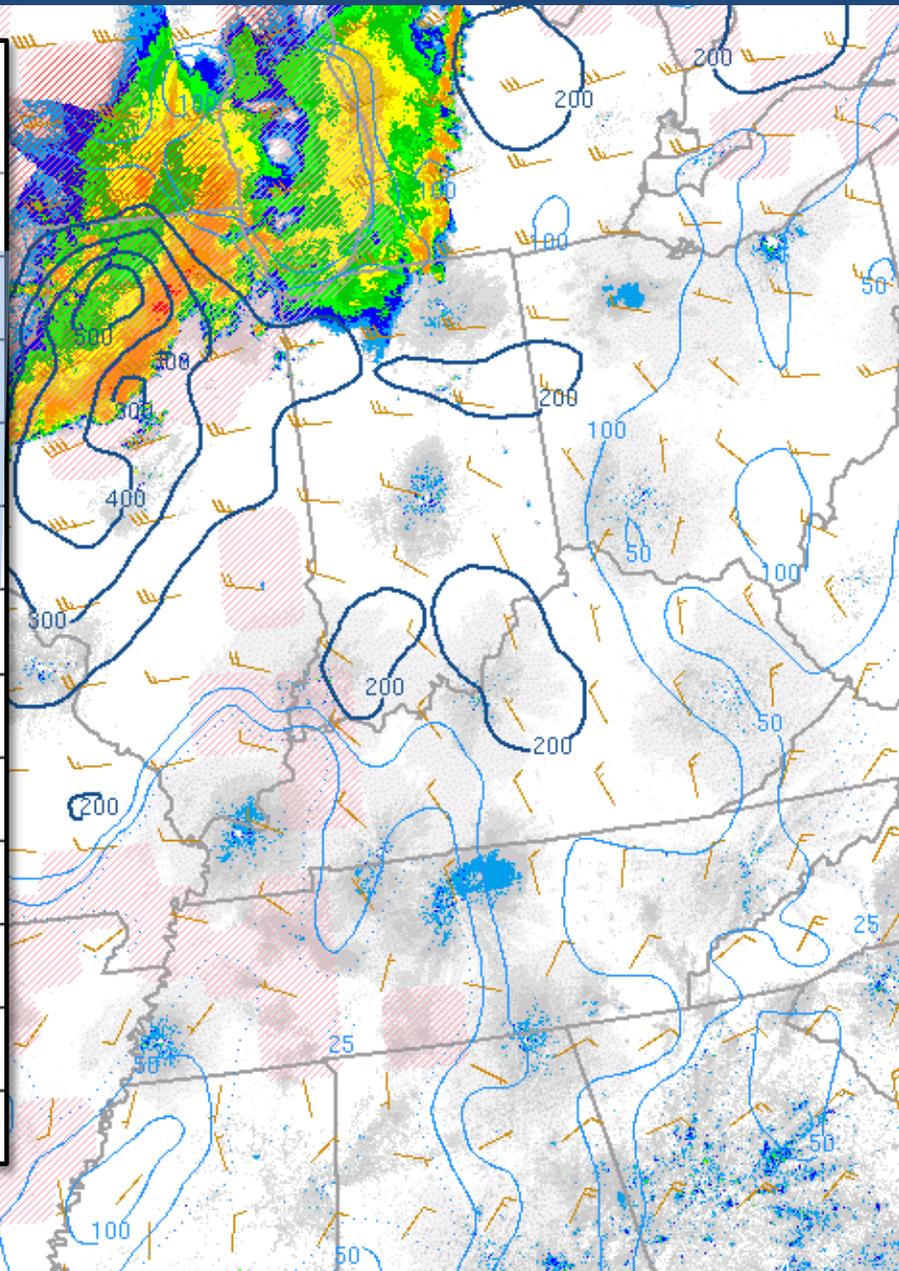
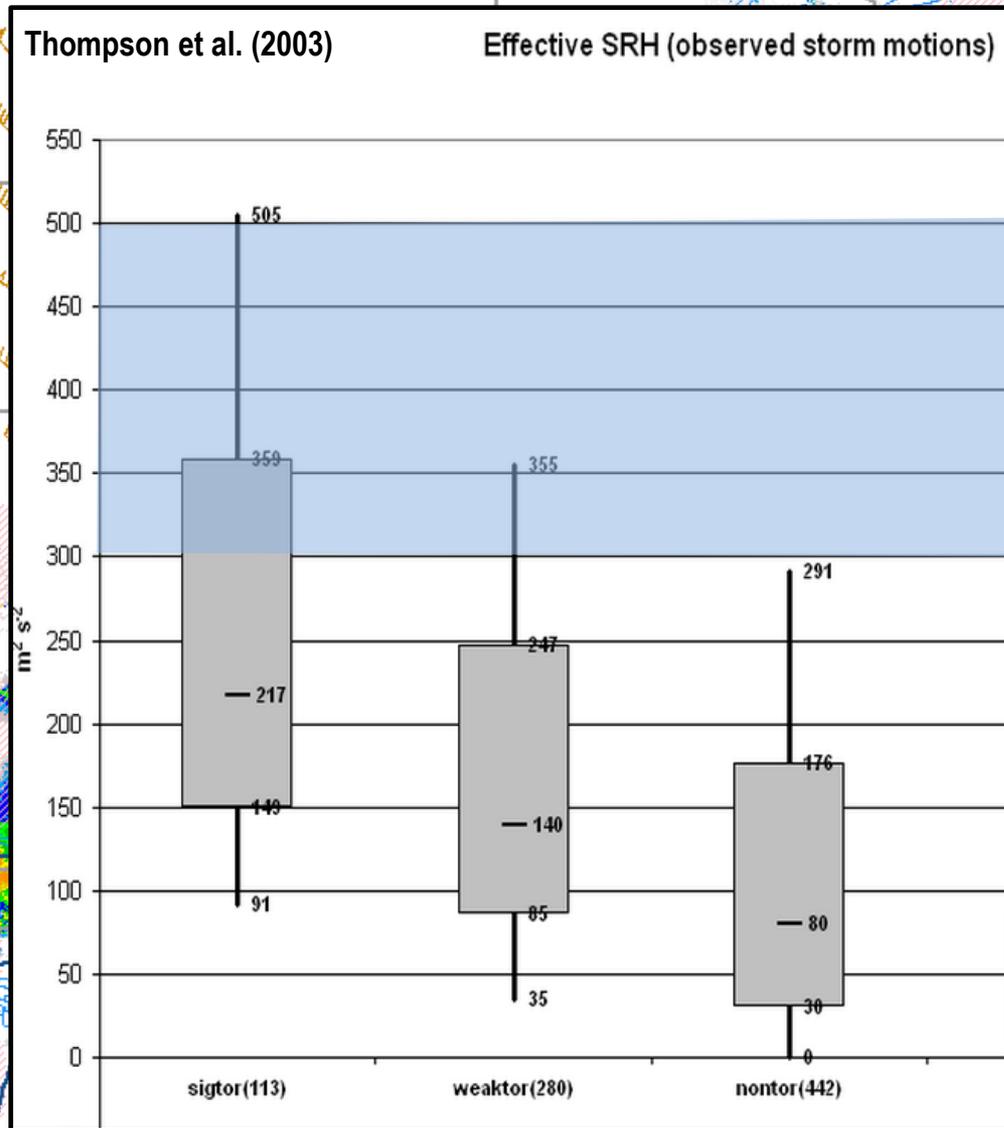
Mesoscale Environment of 30 June 2014: Effective SRH



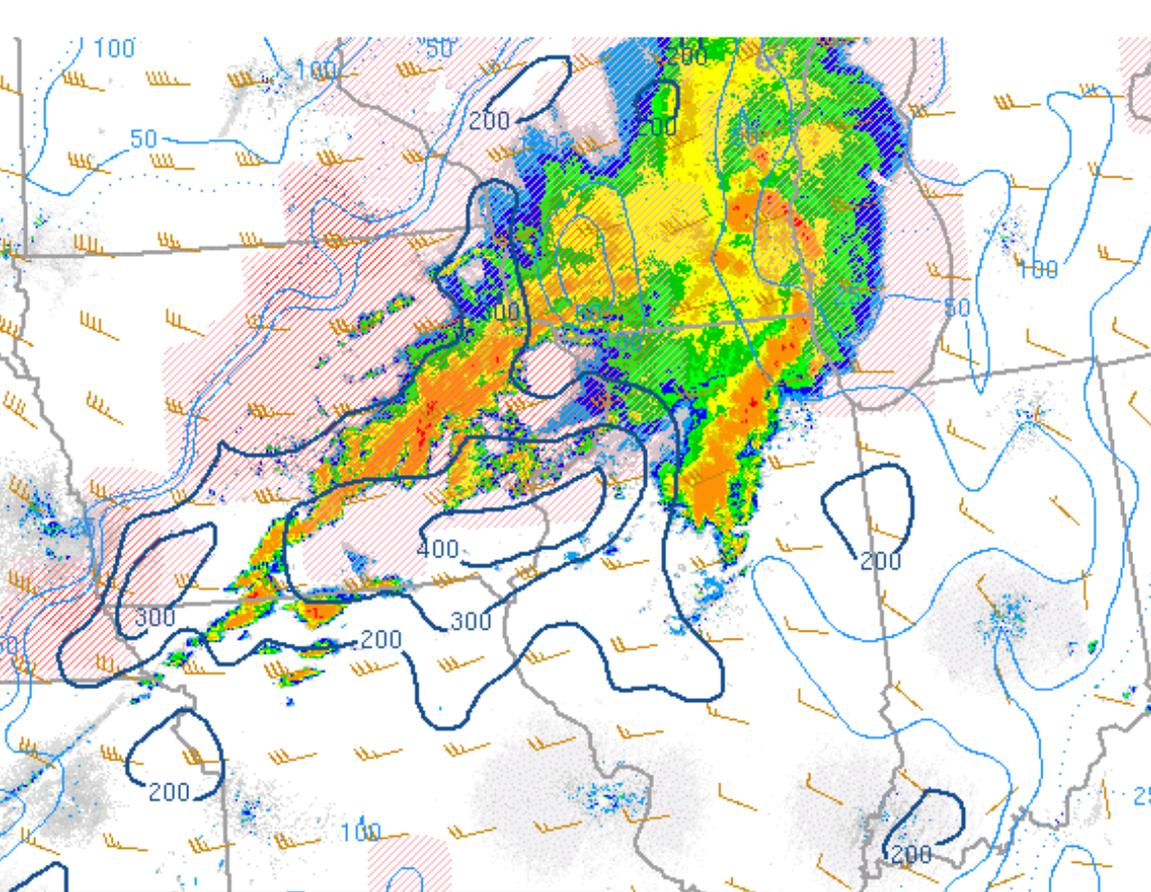
9 pm

140701/0200 Eff. Inflow Base (fill, m AGL), ESRH (m²/s²) and storm motion (kt)

The Synoptic Environment of 30 June 2014: Effective SRH

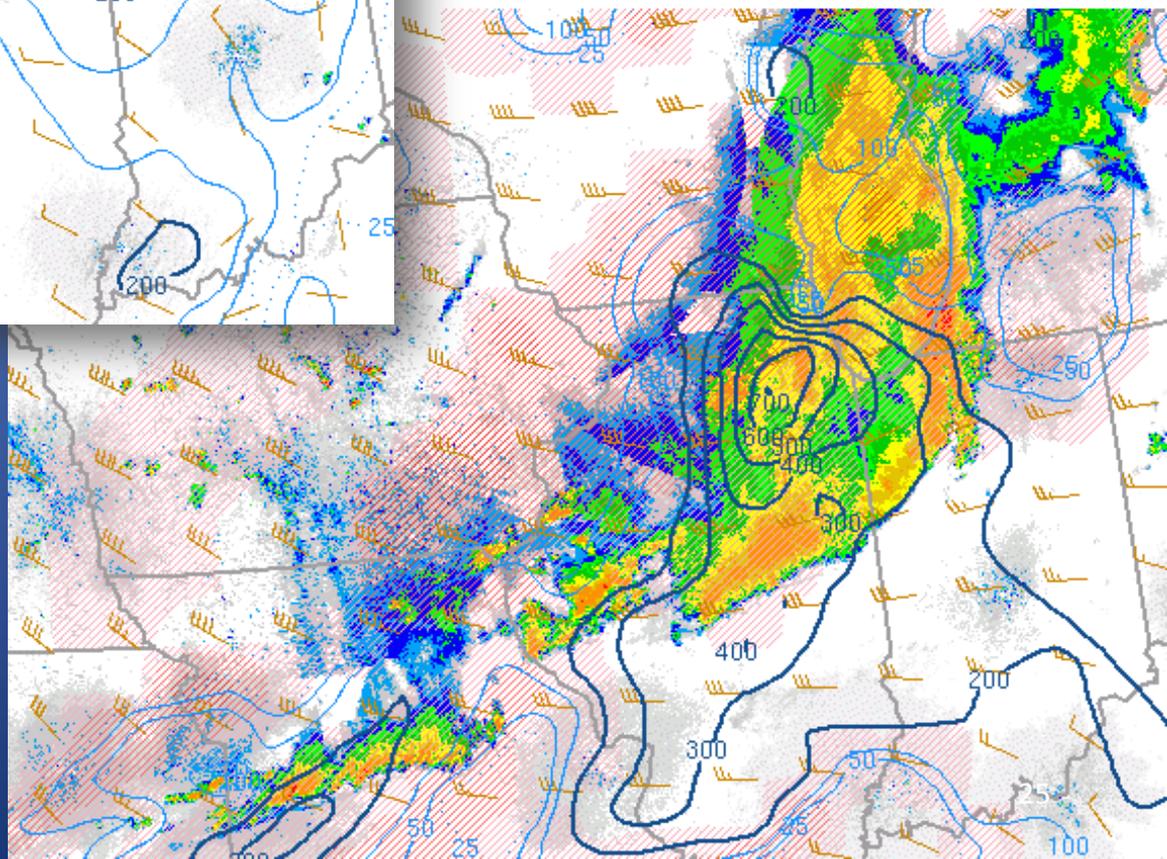


9 pm

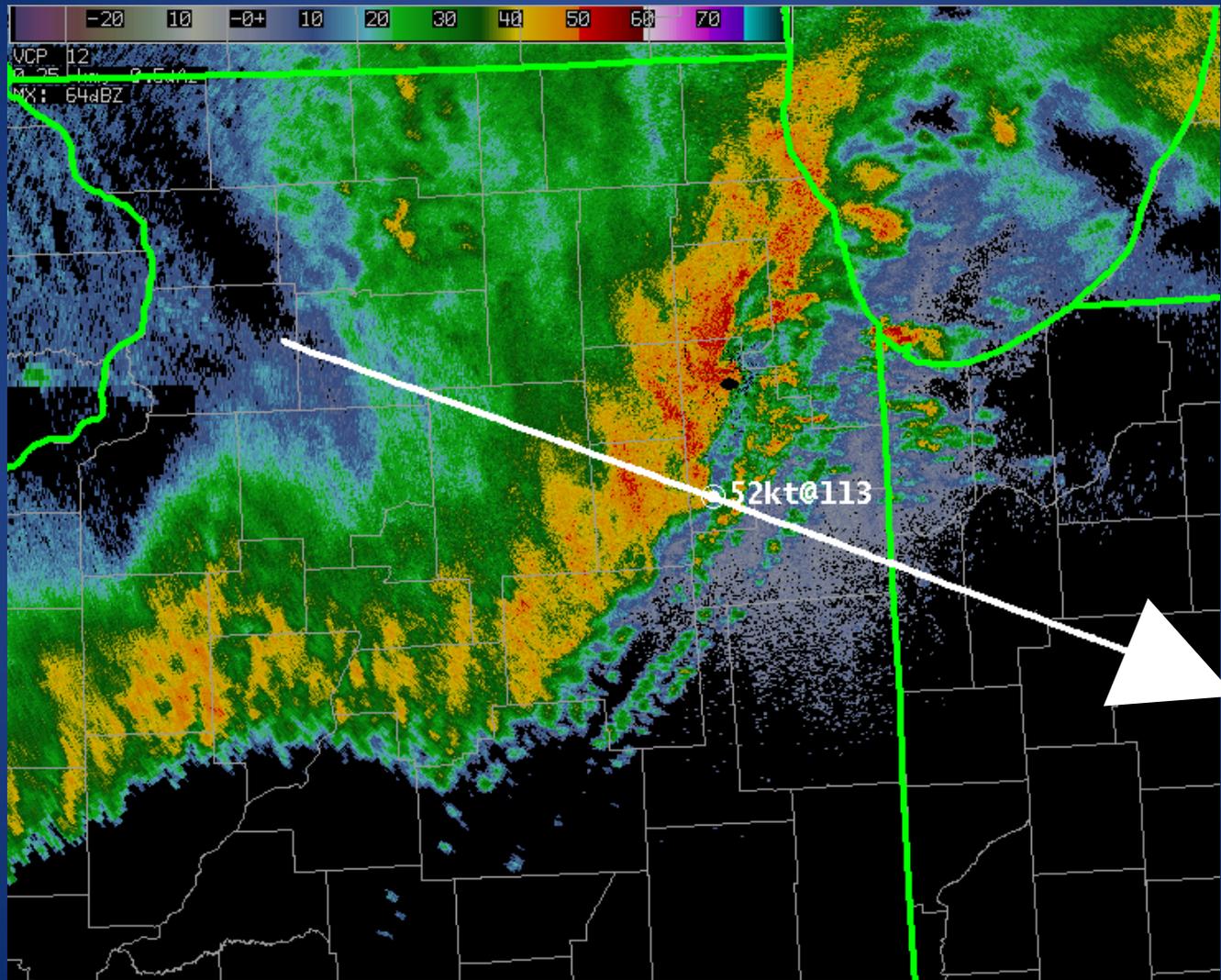


SECOND LINE
04Z Effective SRH:
300-700 m²/s²

FIRST LINE
23Z Effective SRH:
100-200 m²/s²



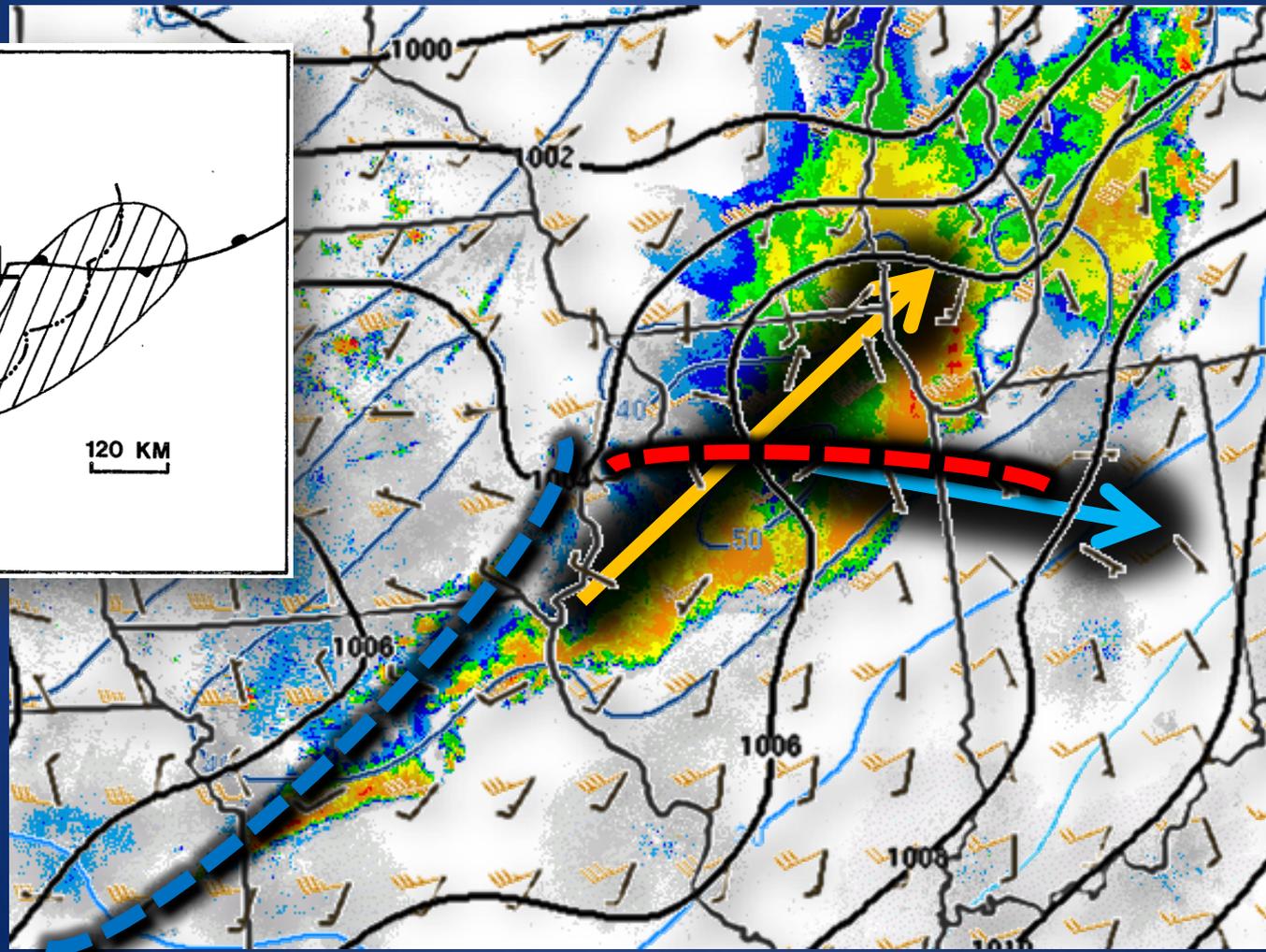
Motion of Tornadic Section of 2nd QLCS

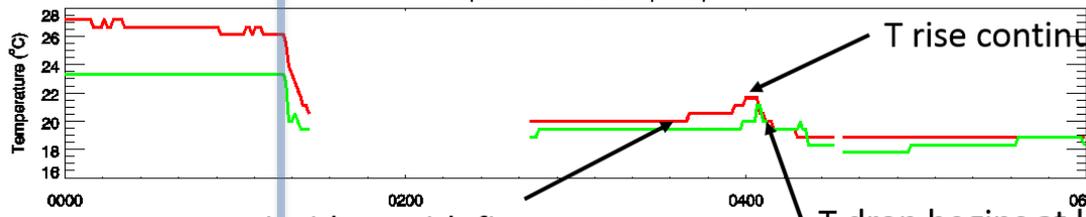


03Z – 1 July 2014

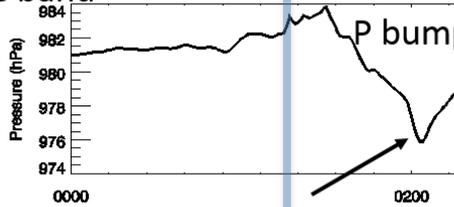
Estimated Motion (27 m/s or 52kt)

850-300mb Mean Wind vs Storm Motion

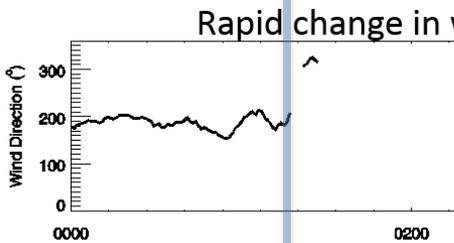
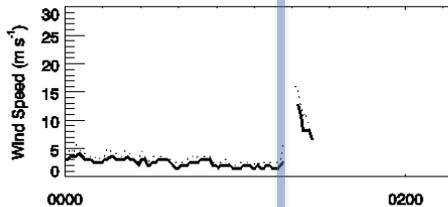




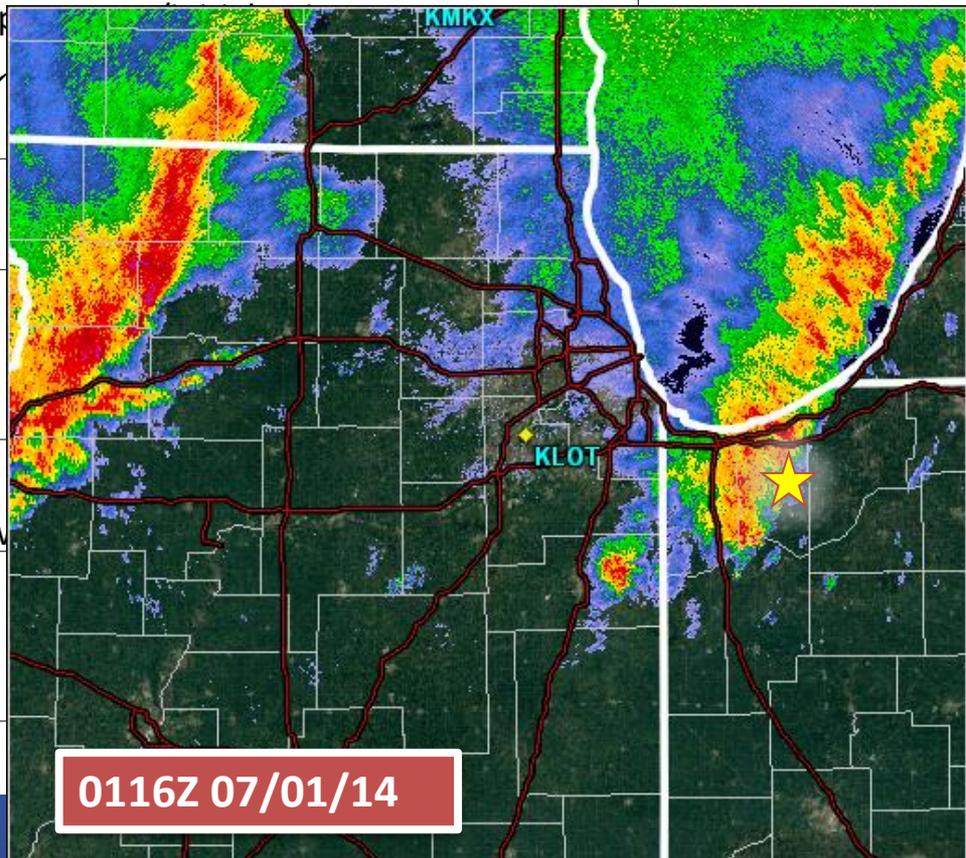
T rise began at 0340 UTC coincident with first convective band
 T rise continues as rapid P rise occurs
 T drop begins at least 2 min after precip begins (Precip at 0402 UTC, T drop at 0404-0405 UTC)



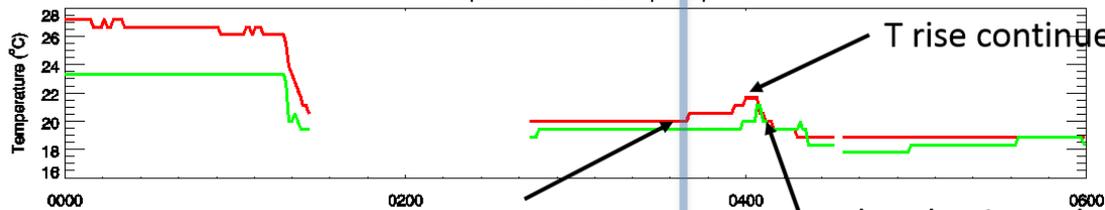
(Side note: wake low passage ~0200 UTC)



Rapid change in v



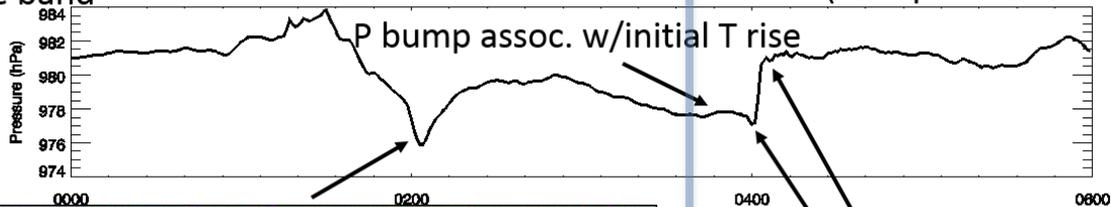
VPZ Time Series



T rise continues as rapid P rise occurs

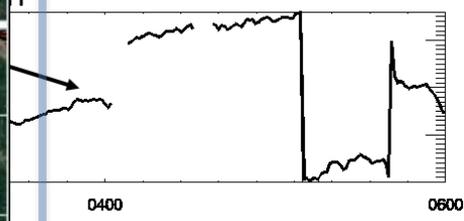
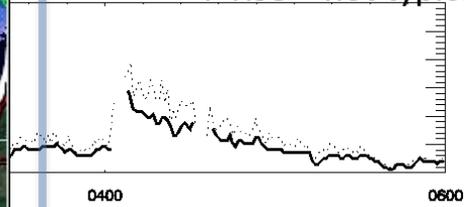
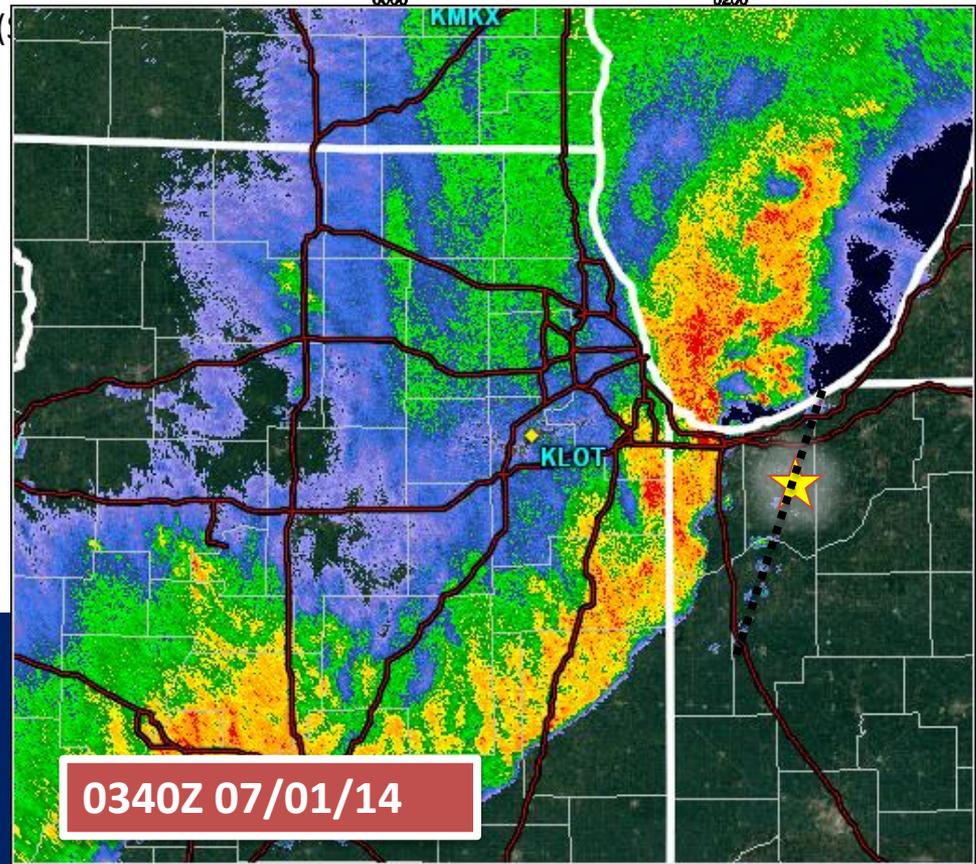
T rise began at 0340 UTC coincident with first convective band

T drop begins at least 2 min after precip begins (Precip at 0402 UTC, T drop at 0404-0405 UTC)

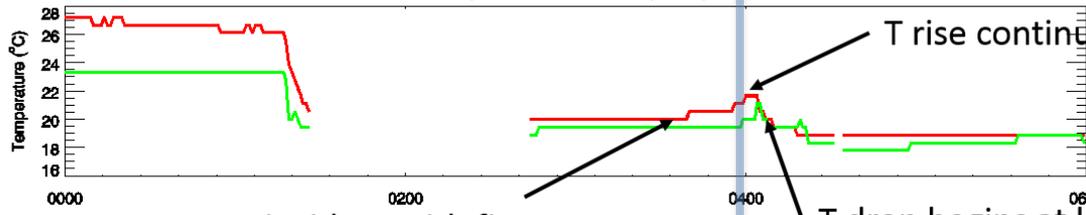


P bump assoc. w/initial T rise

P drop followed by extremely sharp P rise – not typical of a cold pool



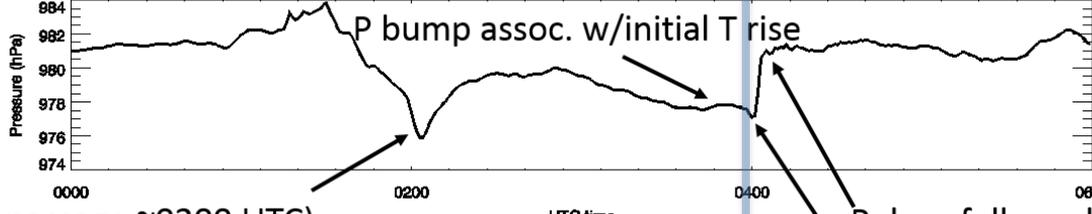
Series



T rise continues as rapid P rise occurs

T rise began at 0340 UTC coincident with first convective band

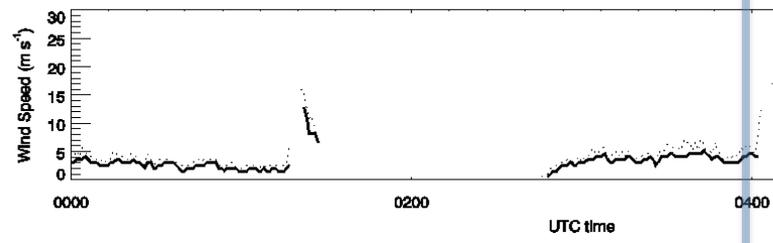
T drop begins at least 2 min after precip begins (Precip at 0402 UTC, T drop at 0404-0405 UTC)



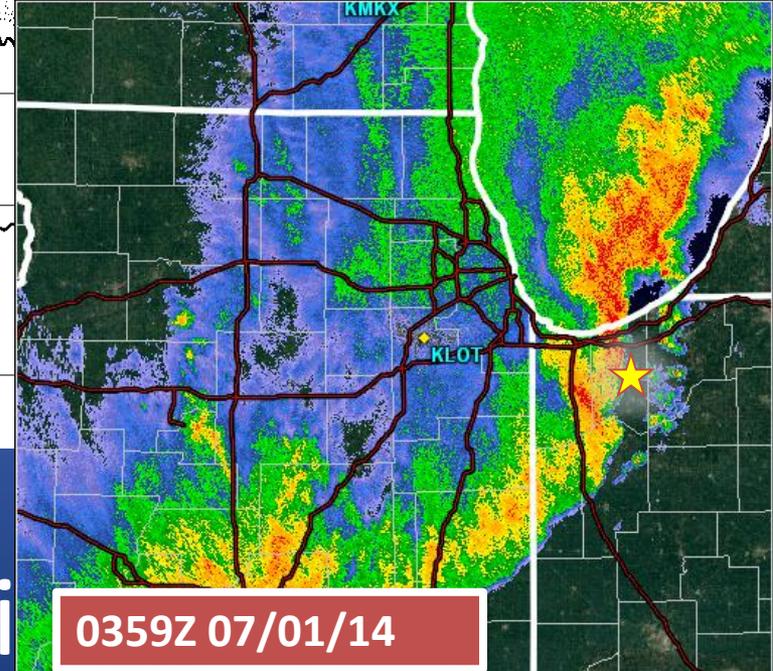
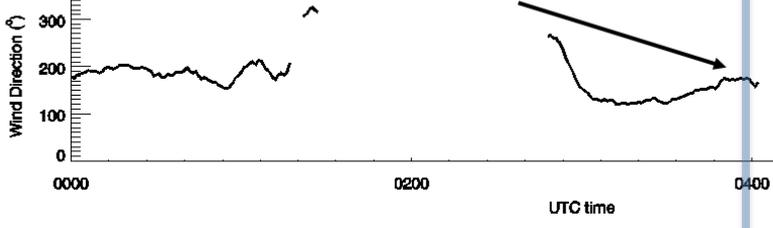
P bump assoc. w/initial T rise

(Side note: wake low passage ~0200 UTC)

P drop followed by extremely sharp P rise – not typical of a cold pool

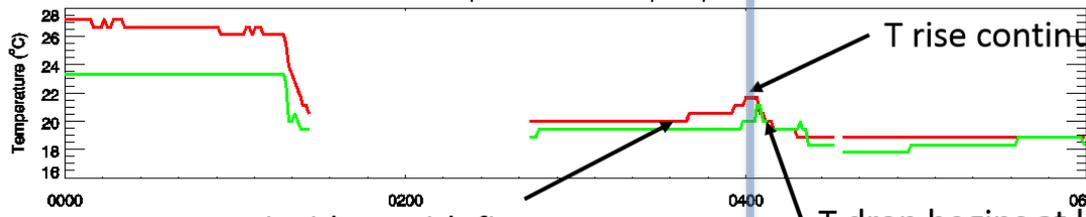


Rapid change in wind direction



VPZ Time Series

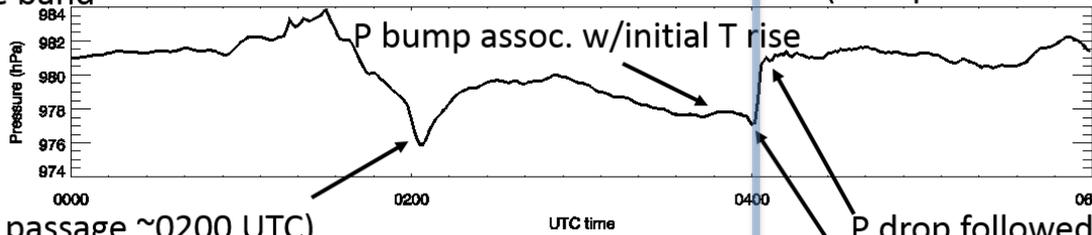
0359Z 07/01/14



T rise continues as rapid P rise occurs

T rise began at 0340 UTC coincident with first convective band

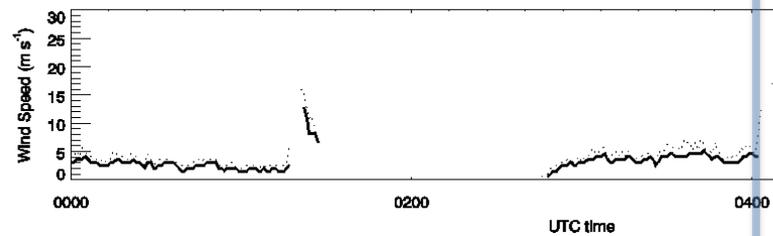
T drop begins at least 2 min after precip begins (Precip at 0402 UTC, T drop at 0404-0405 UTC)



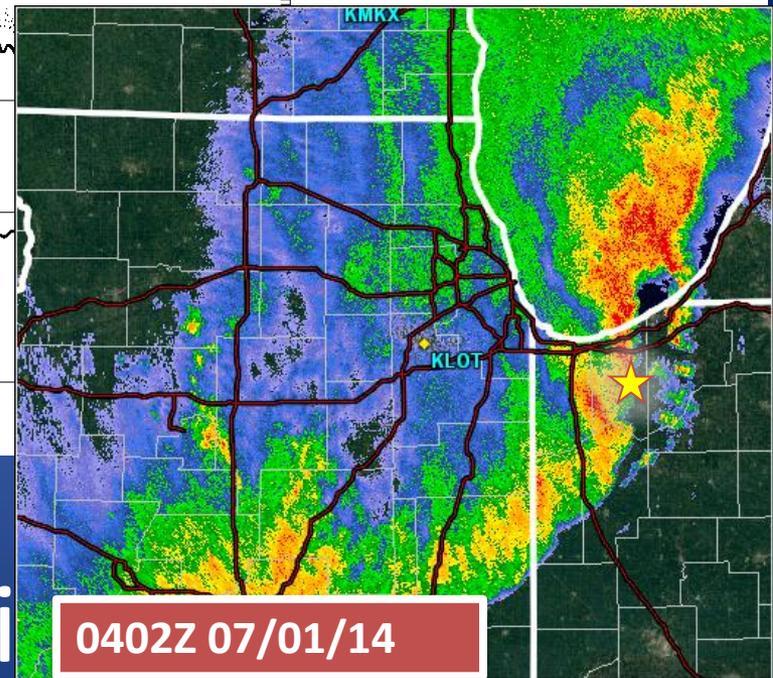
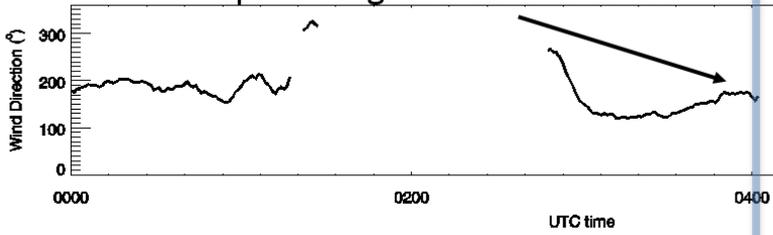
P bump assoc. w/initial T rise

(Side note: wake low passage ~0200 UTC)

P drop followed by extremely sharp P rise – not typical of a cold pool



Rapid change in wind direction



VPZ Time Series

Bore Observations & Dynamics

- TEMPERATURE: Steady or rising
- MIXING RATIO: Steady or decreasing
- PRESSURE: Rapid rise

Destabilization of Boundary Layer

- Common consequence of bores
- Raise inversion height
- Mix warmer, drier air to surface

Temperature rise just ahead of QLCS arrival

**Speed of Density Current
(shallow, with drag)**

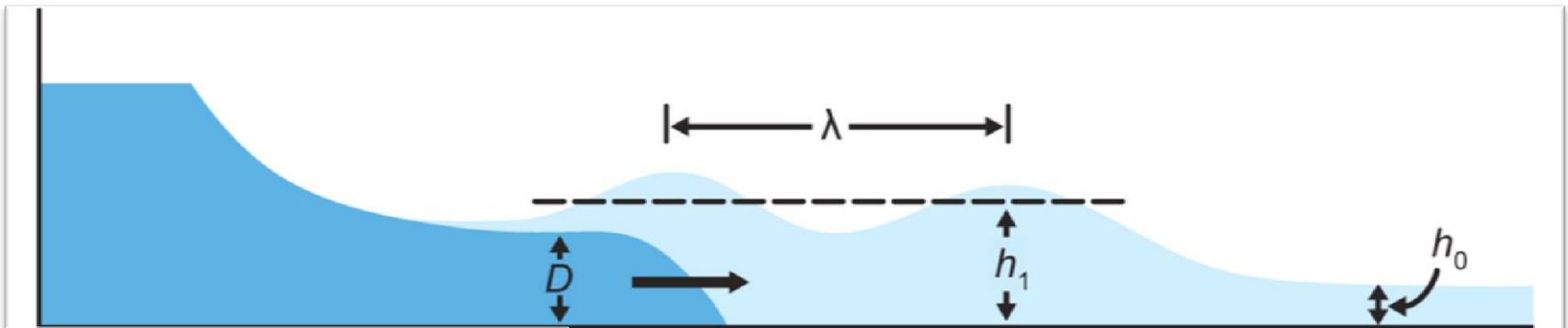
$$c = k \left[gh \frac{\rho_1 - \rho_0}{\rho_0} \right]^{\frac{1}{2}}$$

Speed of Gravity Wave

$$C_{gw} = \left[g \left(\frac{\Delta\theta v}{\theta v} \right) h_0 \right]^{\frac{1}{2}}$$

Speed of Bore

$$C_{bore} = C_{gw} \left[\frac{1}{2} \frac{h_1}{h_0} \left(1 + \frac{h_1}{h_0} \right) \right]^{\frac{1}{2}}$$



Markowski and Richardson 2010

Figure 6.12

Generation of a bore of depth h_1 , by an advancing density current of depth D , intruding into a stable layer of depth h_0 . Shading indicates the density of the fluid, with darker shading indicating denser fluid. (Adapted from Rottman and Simpson [1989].)

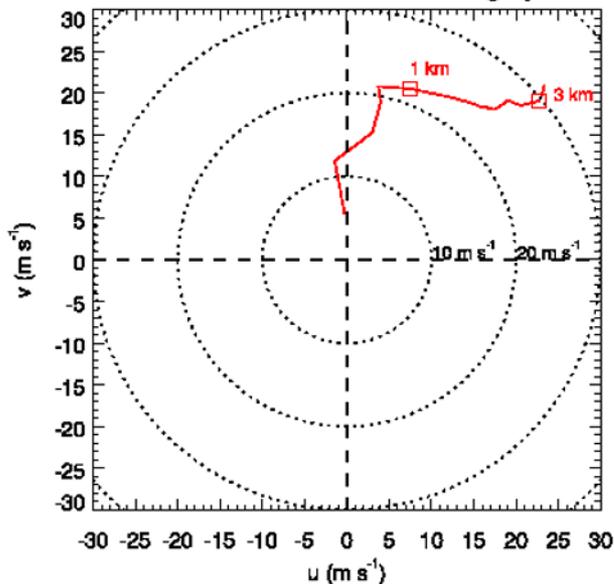
System Motions thru VPZ Area

	1 st QLCS	2 nd QLCS
Actual Speed	17 m/s	25 m/s
Theoretical Cold Pool Speed	16-30 m/s	9-17 m/s
Theoretical Bore Speed	n/a	26 m/s

Bore-Driven Enhancement of SRH

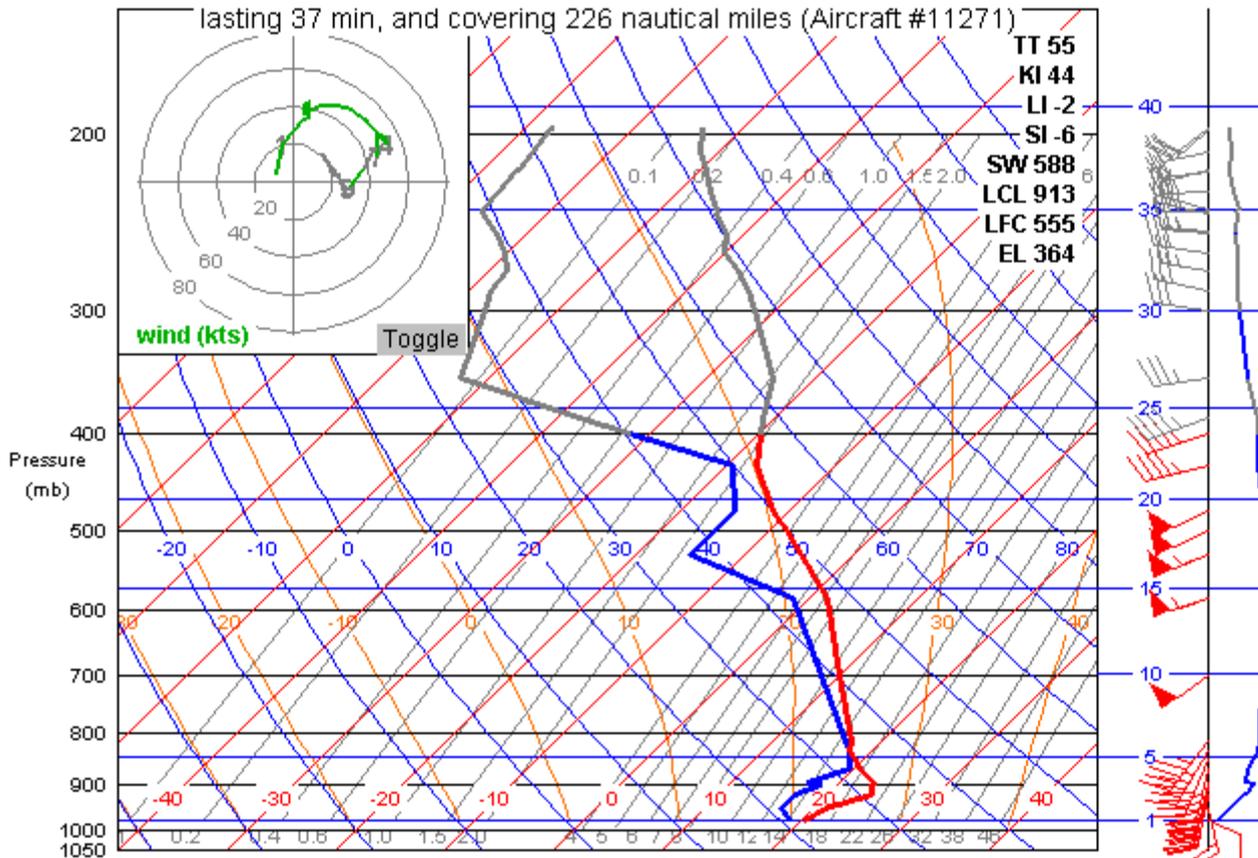
- SRH large even with cold-pool propagation speed
- Faster bore-related movement substantially increased environmental SRH
- Result: SRH was extreme for this QLCS

0249 UTC KLOT EVAD Hodograph

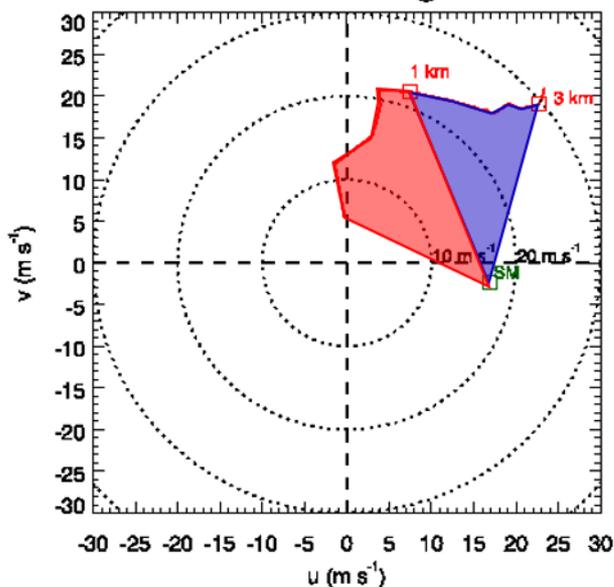


Storm Motion = $278^\circ @ 9 \text{ m s}^{-1}$

Descent sounding from 219° into Chicago/Midway, IL (MDW)
 lasting 37 min, and covering 226 nautical miles (Aircraft #11271)



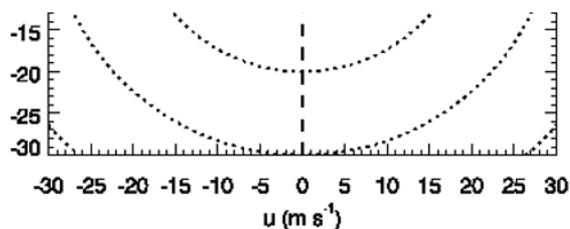
Storm Motion = $278^\circ @ 17 \text{ m s}^{-1}$



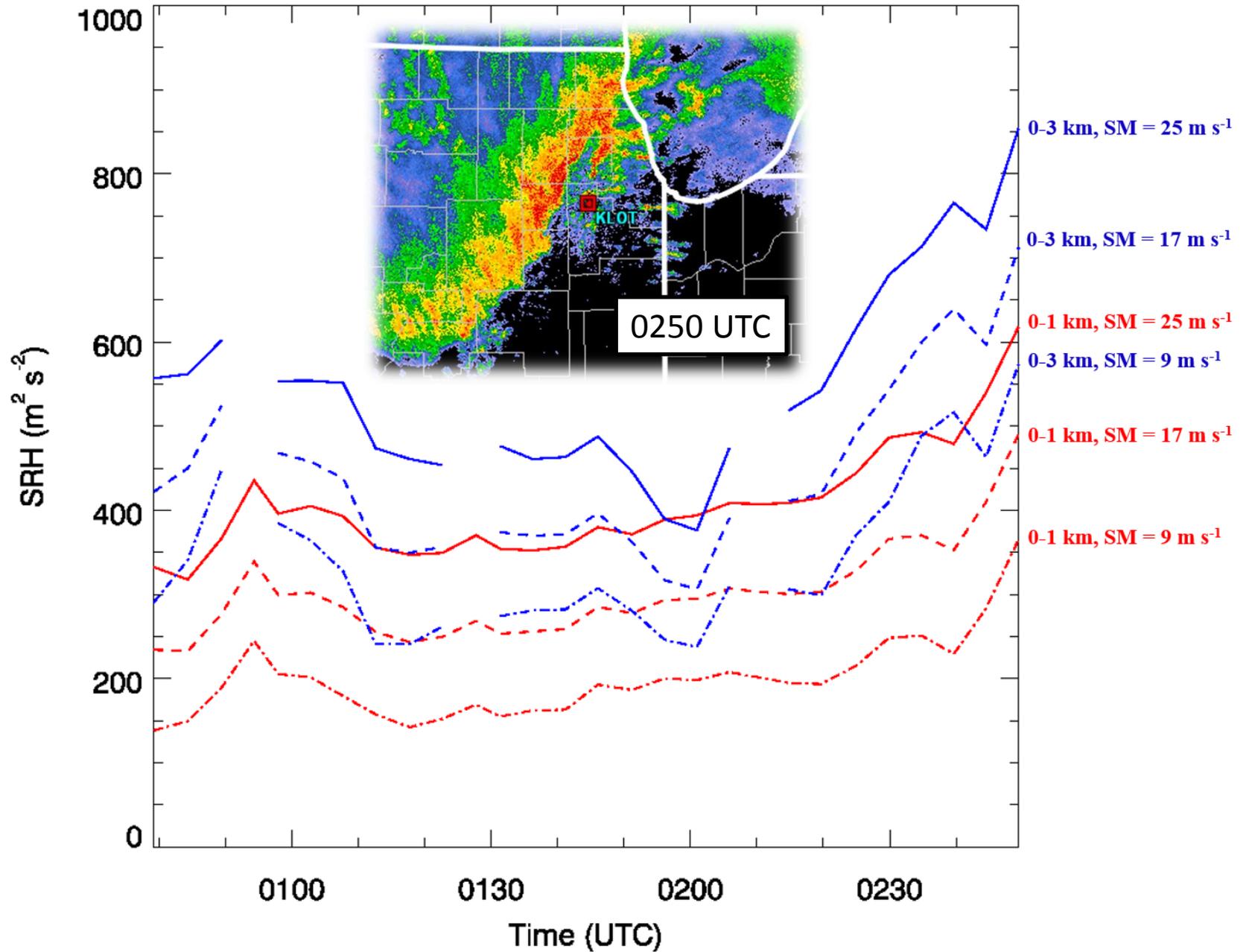
MDW(Dn) 0237 1Jul14 (#11271)

SkewT-log P

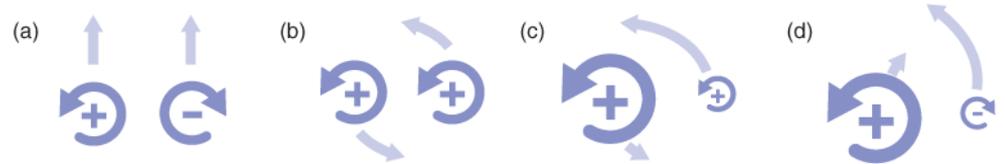
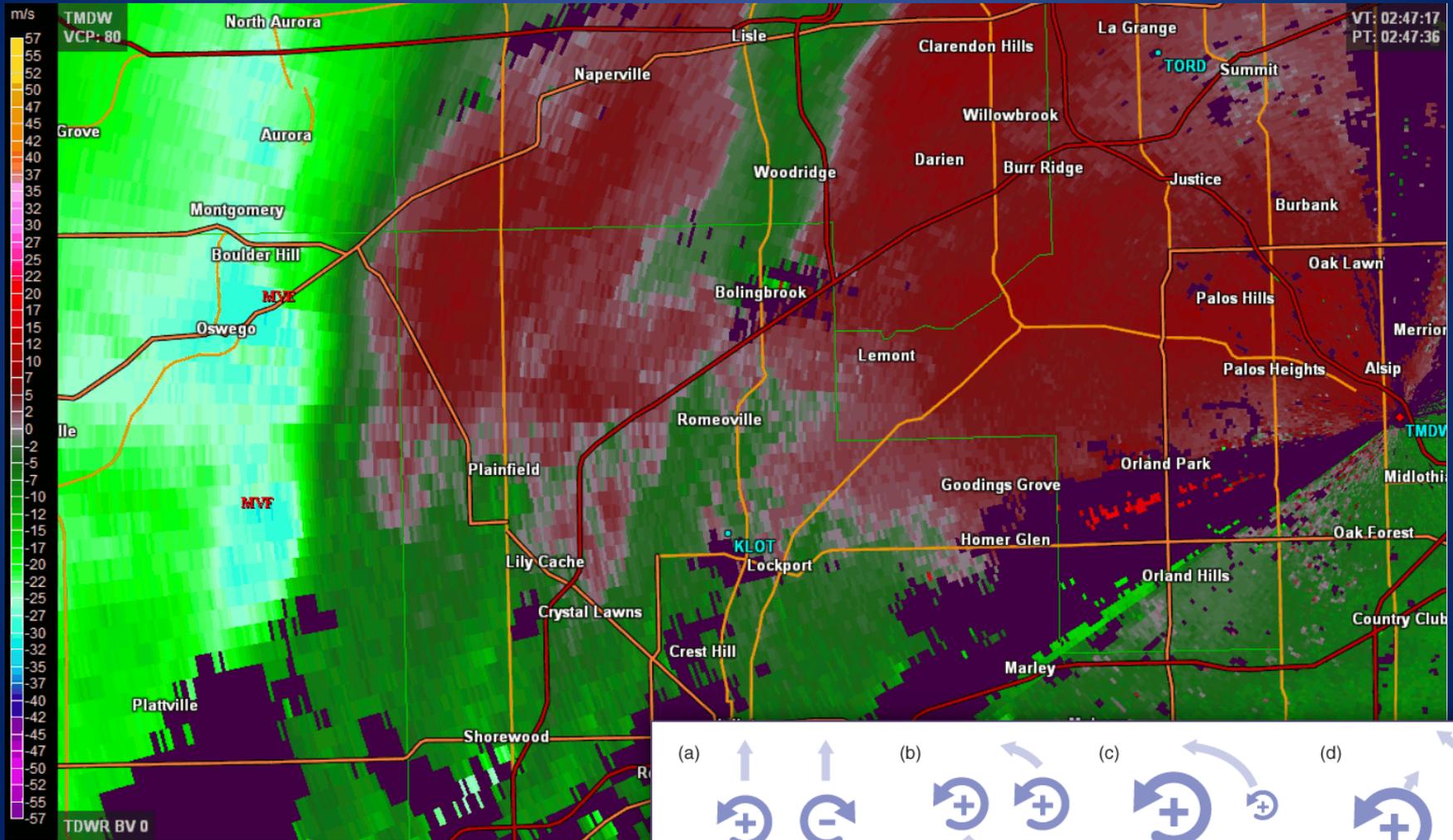
NOAA / ESRL / GSD



KLOT Storm-Relative Helicity



KLOT Close-up View of QLCS Tornado



Fujiwhara Interactions?

Figure 3.17

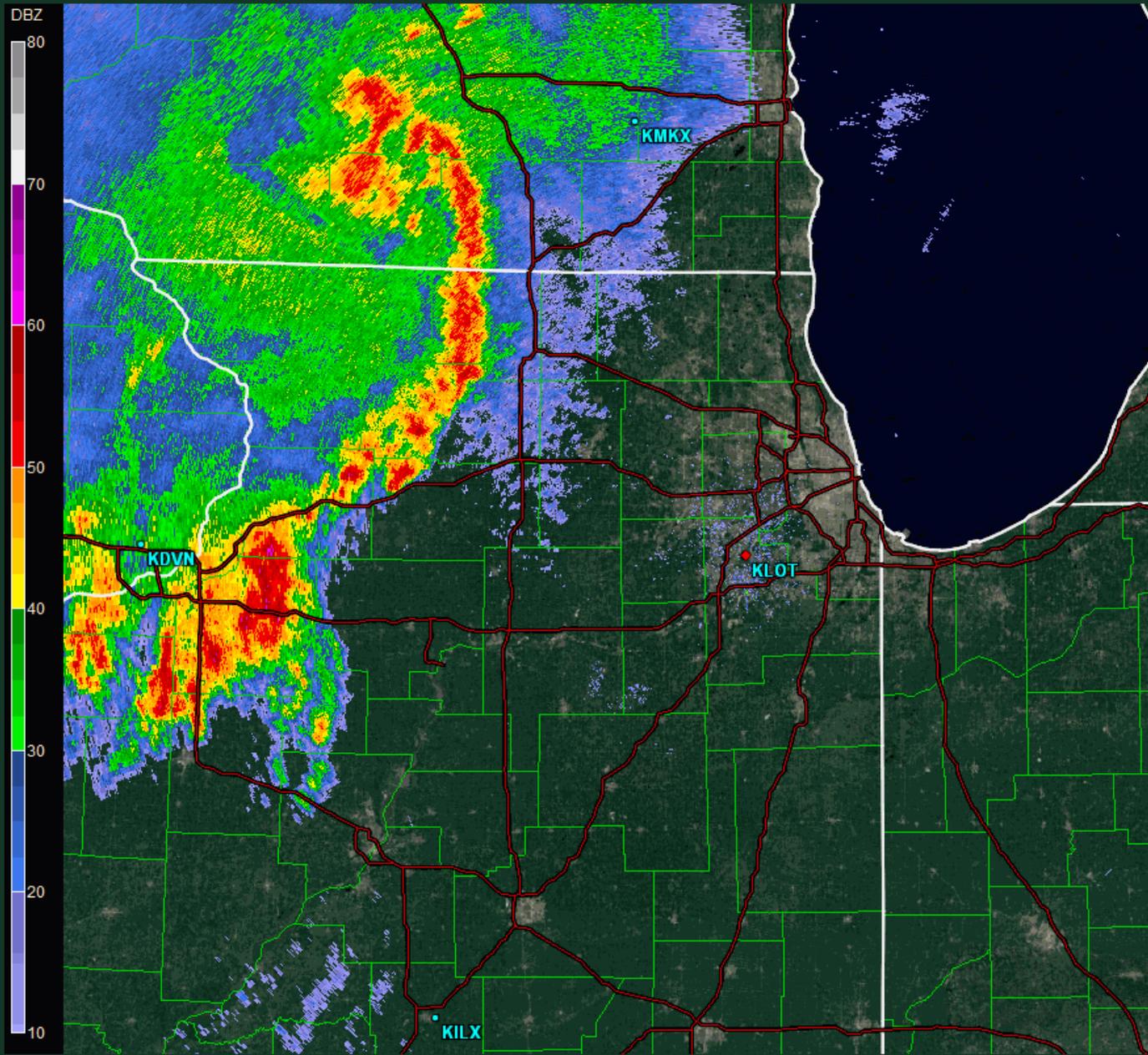
Overall Effect of Bore-Driven Motion

- Ingest of surface or near-surface parcels via:
 - Low-level destabilization
 - Vertical motion associated with bore
- Lifting of parcels to top of stable layer
- Extreme SRH from veered/faster storm motion

Eric.Lenning@noaa.gov

BarryButlerPhotography.com





Site: KLOT
 VST: 06/30/2014 22:01:17 Z
 Prod: 06/30/2014 22:01:16 Z
 VCP: 12 SMV: ----
 Tilt: 0.506°

Select Product:

<input checked="" type="radio"/> BR	<input type="radio"/> VIL	<input type="radio"/> ZDR
<input type="radio"/> BV	<input type="radio"/> VILD	<input type="radio"/> CC
<input type="radio"/> SRV	<input type="radio"/> PQSH	<input type="radio"/> PHI
<input type="radio"/> SW	<input type="radio"/> MEHS	<input type="radio"/> KDP
<input type="radio"/> ET	<input type="radio"/> NROT	<input type="radio"/> HCA

Select Tilt:

0.5°	0.9°	1.3°	1.8°
2.4°	3.1°	4.0°	5.1°
6.4°	8.0°	10.0°	12.5°
15.6°	19.5°		

Product Details:

Max: 64.5 dbz
 Az: 270.2°
 Ran: 87.1 nm